**People's Democratic Republic of Algeria**
**Ministry of Higher Education and Scientific Research**

**University M'Hamed BOUGARA – Boumerdes**


**Institute of Electrical and Electronic Engineering**

**Department of Electronics**

Final Year Project Report Presented in Partial Fulfilment of the Requirements for the Degree of

# MASTER

In **Electrical and Electronic Engineering**

Option: **Telecommunications**

Title:

# Study and Simulation of the Link Adaptation Technology in the LTE Standard

Presented by:

- **MEZIANE Mokrane**
- **ALLILAT Fetta**

Supervisor:

**Mr. Abdelkader ZITOUNI**

Registration Number: 2015/2016

## Dedication

*I have the honor to dedicate this work for my beloved parents Smail and Aladja who have always been the source of all my motivations. To my brothers Brahim, Moh, Hocine,Samir, Mustpha and my sister Hinda with whom I have shared every tiny little experience of my life. They have protected me and opened up for our familly a stream of succes along the way.*

*A speciale dedication goes to all my friends, as far or close they may be, to all the amazing people I have met from all over the world.*

*I have a speciale though for my best friends Farid and Yacine*.

*Meziane Mokrane*.

## Dedication

*First and foremost I would like to thank God for givig me the power to believe in my passion and pursue my dreams.*

*I dedicate this work to my loving parents, special feeling of gratitude for you father Rachid and mother Fadhila, your words of encouragement and push for tenacity ring in my ears. To my beloved brothers and sisters, Tassadit, Mhend and Ounissa thank you for being a part of my life.*

*To my one and only Sebaa Mohamed, I give my deepest expression of love and appreciation for the encouragements you gave, the sacrifices you made and the support you provide.*

*To all my friends and all the great people that I knew during this graduation program, thank you for your friendship, your advices, your help and support.*

*Fetta Allilat*

## Acknowledgment

First of all our sincer considerations goes to our supervisor Dr. A.ZITOUNI for the guidance and the help he provided. For his encouragement along the way to satisfy our eagersness to explore additional areas. We are very grateful for the opportunity he gave us to learn a new field, work on an interesting topic and meet a number of wonderful people along the way.

We would also like to thank our mentors at Huawei Telecom Mr B.DEBAGHI who often made himself available despite all the pressure he is facing daily. He greatly inspired us with his tremendous passion for this field. Thank you for the wonderful conversations and the opportunity to learn and work with you. Thank you to Huawei for supporting this thesis and generously allowing us to explore and have an insight of the professional life and meet highly skilled people in this field.

Never the less we would like to thank the IGEE stuff, the teachers, the administration staff and the security teams for their help support and the way they made this experience exceptional.

## Abstract

The Long Term Evolution first introduced by the link adaptation system as a massive step forward in the control of the network resources. It is mainly based on measuring instantaneous Signal to Interference and Noise Ratio (SINR) which is used to investigated the influence of several parameters on the link adaptation error characteristics. Adaptive Modulation and Coding (AMC) is used to increase the network capacity or downlink data rates. Spatial multiplexing techniques for MIMO antenna configurations are also considered.

This report has outlined the various scheduling techniques used in the link adaptation process to increase the throughput of the network. Three major channel state report measurements are used to perform the adaptations which are: CQI (channel quality indicator), PMI (Precoding Matrix Indicator), and RI (Rank Indicator) measurements.

An analysis and a comparison of these scheduling algorithms were done through simulations executed on MATLAB software. The impact of the scheduling schemes was examined on the throughput (Average Data Rate) and the Bit Error Rate (BER), and it was compared to the case where no adaptation is done.

The fairness of the results given by each scheduling scheme was investigated. The link adaptation improved the transmission robustness through minimizing the error and increased the spectral efficiency to produce a satisfactory average data.

## Table of contents

Dedication ..... I

Acknowledgment ..... III

Abstract ..... IV

Table of contents ..... V

List of Tables ..... VIII

List of figures ..... X

List of Abreviations ..... XII

Introduction ..... 1

1. LTE Standard Physical layer ..... 3

1.1 LTE Network Architecture ..... 3

1.1.1 Frequency bands ..... 4

1.1.2 Time framing ..... 4

1.1.3 Time–Frequency Representation ..... 5

1.1.4 Resource grid content ..... 5

1.1.5 Physical Channels and Physical Signals ..... 7

1.1.5.1 Downlink Pysical channels ..... 8

1.1.5.2 Uplink Physical channels ..... 9

1.2 LTE enabling technologies ..... 10

1.2.1 OFDM ..... 10

1.2.1.1 Downlink: Orthogonal Frequency Division Multiple Access (OFDMA) ..... 11

1.2.1.2 Uplink: Single-Carrier Frequency Division Multiple Access (SCFDMA) ..... 11

1.2.1.3 OFDM Transmitter Chain ..... 12

1.2.2 Channel Coding ..... 12

1.2.3 MIMO ..... 14

1.2.3.1 MIMO Channel ..... 14
1.2.3.2 MIMO Receiver ..... 15
1.2.3.3 Transmission modes in LTE downlink ..... 16
1.2.4 Link Adaptation ..... 17
1.3 Physical Layer Processing ..... 17
1.3.1 Downlink Processing ..... 17
Conclusion ..... 19
2. Link Adaptation in LTE ..... 20
Introduction ..... 20
2.1 System Model ..... 20
2.2 Channel-state report for Link Adaptation ..... 22
2.2.1 Channel Quality Indicator ..... 22
2.2.2 Precoding Matrix Estimation: ..... 24
2.2.3 Rank Estimation: ..... 28
2.3 Work description: ..... 28
3. Simulation and Results ..... 29
Introduction ..... 29
3.1 Simulation Model Description ..... 29
3.2 CQI Based Adaptation ..... 31
3.2.1 No Adaptation ..... 31
3.2.2 Adaptive Modulation ..... 33
3.2.3 Adaptive modulation and coding ..... 36
3.3 PMI and RI Based Adaptation ..... 40
3.3.1 PMI Based Adaptation ..... 40
3.3.2 RI & PMI Based Adaptation ..... 42

1. Part A: ..... 42
2. Part B: ..... 46
3.4 Adaptation Based on CQI, PMI and RI ..... 48
3.5 Results Summary ..... 52
Conclusion ..... 53
General Conclusion ..... 54
Future Work ..... 55
References ..... XII

# List of Tables

## Chapter I LTE Standard Physical Layer

**Table1. 1: LTE Uplink/Downlink Throughput Speeds. 1**

**Table1. 2: Channel bandwidth specified in lte. 4**

**Table1. 3: LTE downlink physical channels. 8**

**Table1. 4: LTE uplink physical channels. 9**

## Chapter II Link Adaptation

**Table2. 1: Lookup table for mapping SINR estimate to modulation scheme and coding rate. 24**

**Table2. 2: Precoding matrices for two transmit antennas in LTE spatial multiplexing. 26**

**Table2. 3: Precoding matrices for four transmit antennas in LTE spatial multiplexing. 27**

## Chapter III Simulation and Results

**Table 3. 1: Channel parameters. 31**

**Table3. 2: Number of subframes and average data rate for each modulation. 33**

**Table3. 3: Results for the adaptive and non-adaptive modulation experiment. 35**

**Table3. 4: SNR to CQI mapping for adaptive modulation 36**

**Table3. 5: Results for non-adaptive and adaptive modulation and coding scheme 38**

**Table3. 6: SNR measured mapped to CQI index and modulation with coding rate 39**

**Table3. 7: Channel parameters 40**

**Table3. 8: Results for adaptive PMI based simulation and the no adaptation simulation 41**

**Table3. 9: Channel parameters 42**

**Table3. 10: Results for the mode 2 transmit diversity and mode 4 spatial multiplexing 44**

**Table3. 11: Results for the two modes and the adaptatin based on the RI estimation 45**

**Table3. 12: Results for PMI+RI adaptation, PMI adaptation and no adaptation case 47**

**Table3. 13: Channel parameters for a 2*2 transceivers 48**

**Table3. 14: Channel parameters for the 4*4 transceiver 50**

**Table3. 15: Results for the 4*4 MIMO transciever 51**

**Table3. 16: Comparative results for adaptive modulation 52**

**Table3. 17: Comparative results for adaptive modulation and coding 52**

**Table3. 18: Comparative results for adaptive PMI with no adaptation..... 52**

**Table3. 19: Comparative results for the fixed mode 2 and 4 with adaptive mode ..... 53**

**Table3. 20: Comparative results for the PMI+Ri based adaptation..... 53**

# List of figures

## Chapter I LTE Standard Physical Layer


**Figure 1. 1: The interfaces between the differe²nt parts of the system. ..... 3**

**Figure 1. 2: The architecture of the E−UTRAN . ..... 3**

**Figure 1. 3: LTE time domain structure. ..... 5**

**Figure 1. 4: Resource elements, blocks and grid. ..... 6**

**Figure 1. 5: Physical channel and signal content of LTE downlink subframe in unicast mode. ..... 7**

**Figure 1. 6: Layer architecture in a LTE radio access network. ..... 7**

**Figure 1. 7: Mapping LTE downlink logical, transport, and physical channel. ..... 9**

**Figure 1. 8: Mapping LTE uplink logical, transport, and physical channels ..... 10**

**Figure 1. 9: The spectrum of multiple truncated modulated OFDM subcarriers with constant amplitude. ..... 10**

**Figure 1. 10 : Subcarrier allocation in OFDM and OFDMA. ..... 11**

**Figure 1. 11 : Transmission of a series of QPSK symbols in both OFDMA and SC-FDMA. ..... 11**

**Figure 1. 12: LTE OFDM Transmitter Chain with Modulation and Coding, IFFT and CP ..... 12**

**Figure 1. 13: Block Diagram of the LTE Turbo Encoder. ..... 13**

**Figure 1. 14 : Signal processing chain of downlink DLSCH and PDSCH. ..... 18**


## Chapter II Link Adaptation


**Figure 2. 1 : Sequence of downlink and uplink operations involved in link adaptation. ..... 21**

**Figure 2. 2: SNR-CQI mapping model. ..... 23**

**Figure 2. 3: Block diagram of (a) MIMO without precoding and (b) MIMO with precoding. ..... 26**


## Chapter III Simulation and Results


**Figure 3. 1: LTE physical layer model as defined by the standard ..... 29**

**Figure 3. 2: System model for the LTE physical layer ..... 30**

**Figure 3. 3: Report of parameters and measurments by subframe ..... 32**

**Figure 3. 4: Bit Error Rate for the Three Modulations without Adaptation ..... 32**

**Figure 3. 5: parameters and measurements for each subframe ..... 34**

**Figure 3. 6: Bit Error Rate for adaptive and non-adaptive modulation ..... 34**

**Figure 3. 7: Average Data Rate for adaptive a non-adaptive modulation ..... 35**

**Figure 3. 8: paramters and results for each subframe ..... 36**

**Figure 3. 9: Bit Error Rate for adaptive modulation and coding rate with the no adaptation case ..... 37**

**Figure 3. 10: Average Data Rate for non-adaptive and adaptive modulation and coding scheme ..... 38**

**Figure 3. 11: Bit Error Rate for adaptive MCS with the measured SNR for each subfram ..... 39**

**Figure 3. 12: Bit Error Rate for adaptive PMI and no adaptation ..... 41**

**Figure 3. 13: Bit Error Rate for the fixed mode 2 transit diversity and the fixed mode 4 spatial multiplexing ..... 43**

**Figure 3. 14: Average Data Rate for the fixed mode 2 transit diversity and the fixed mode 4 spatial multiplexing ..... 43**

**Figure 3. 15: Bit Error Rate for the fixed mode 2 and the fixed mode 4 with the adaption RI based ..... 44**

**Figure 3. 16: Average Data Rate for the fixed mode 2 and the fixed mode 4 with the adaption RI based .. 45**

**Figure 3. 17: Bit Error Rate for the adaptation based PMI+Ri ,PMI based and no adaptation ..... 46**

**Figure 3. 18: Average Data Rate for PMI+RI based adaptation, PMI based adaptation and no adaptation ..... 46**

**Figure 3. 19: Bit Error Rate for a2*2 MIMO transceiverTransceiver and the measured SNR..... 49**

**Figure 3. 20: Average Data Rata for 2*2 MIMO transceiver with the measured SNR ..... 49**

**Figure 3. 21:Bit Error Rate for the 4*4 MIMO transceiver the measured SNR for each subframe ..... 50**

**Figure 3. 22: Average Data Rate for the 4*4 MIMO transceiver the measured SNR for each subframe... 51**

## List of Abreviations

| | |
|---|---|
| **16QAM** | 16-ary quadrature amplitude modulation |
| **3GPP** | 3rd Generation Partnership Project |
| **64QAM** | 64-ary quadrature amplitude modulation |
| **AWGN** | additive white Gaussian |
| **BER** | bit error rate |
| **CQI** | Channel quality information/indicator |
| **eNodeB** | E-UTRAN NodeB |
| **FDD** | Frequency division duplex |
| **LTE** | Long term evolution |
| **MAC** | Medium access control |
| **MIMO** | Multiple-Input Multiple-Output |
| **OFDM** | Orthogonal frequency division multiplexing |
| **PBCH** | Physical broadcast channel |
| **PCFICH** | Physical control format indicator channel |
| **PDCCH** | Physical downlink control channel |
| **PDCP** | Packet data convergence protocol |
| **PDSCH** | Physical downlink shared channel |
| **PHY** | Physical layer |
| **PMCH** | Physical multicast channel |
| **PRACH** | Physical random access channel |
| **PUCCH** | Physical uplink control channel |
| **PUSCH** | Physical uplink shared channel |
| **SC-FDMA** | Single carrier-Frequency division multiple access |
| **SINR** | Signal to interference and noise ratio |
| **SNR** | Signal noise ratio |
| **TDD** | Time division duplex |
| **UE** | Userequipment |

# Introduction

Wireless communications is allowing people to remain connected on a daily basis in ways never seen before. Wireless has enhanced our lives in such a way that we can no longer see ourselves without this technology and we can only speculate on what it might enable next. The next generation of wireless networks promise to deliver more bandwidth and a higher - data rates to the consumer using exciting technologies like multi-antenna wireless systems, Wifi hot spots, pico cells and coordinated multi-point (CoMP) that work with the base station in a wireless radio access network to offload bandwidth from the wireless base stations and increase the consumer experience [1].

Long Term Evolution (LTE) is a new wireless technology developed by the 3rd Generation Partnership Project (3GPP) and first standardized in 3GPP release 8 standards documentation. In 2007, the first release of LTE offered exciting new improvements to wireless access speeds by using orthogonal frequency division multiplexing (OFDM) on the downlink to send data to the consumer and achieve high bit rates. The bit rates achievable by the LTE wireless network downlink are shown in table 1.1.

**Table1. 1: LTE Uplink/Downlink Throughput Speeds.**

| **Downlink speed (Mbps)** | **10** | **50** | **100** | **150** | **300** |
|---|---|---|---|---|---|
| **Uplink speed (Mbps)** | 5 | 25 | 50 | 50 | 75 |
| **Receiver Antennas Required** | 2 | 2 | 2 | 2 | 4 |

The mentioned peak rates are almost never achievable since they require the channel conditions to be good enough to use a high modulation order and little coding redundancy (high code rates). Therefore an error rate criterion is used to select the convenient data rate. This is called link adaptation, which is an integral part of LTE.

In LTE, the link adaptation chooses the Modulation and Coding Scheme (MCS), based on the Signal to Interference and Noise Ratio (SINR) estimates. This estimates are measured on some reference signal as experienced by the receiver. Therefore, the more

accurate the SINR estimation, the better is the link adaptation and the chosen MCS for the prevailing channel conditions. Hence the accuracy of link adaptation directly affects the system throughput [2].

This thesis related to link adaptation showcases the behaviour of this system using MATLAB software implementation.

**Problem Statement**

In the LTE, Link Adaptation performs several scheduling mechanisms in order to improve the system's response, where the User Equipments (UEs) measure the received (SINR) and report to the base station specific signalling that allows it to adapt the modulation and coding scheme MCS, change the number of transmit antennas (adaptive MIMO), and even change the transmission bandwidth (adaptive bandwidth).

The data rate is determined by the chosen MCS and MIMO state where the error rate depends on the MCS and the prevailing channel quality and the MIMO transmission mode. A higher order modulation scheme such as 64QAM or 16QAM would allow more bits per modulation symbol, thus allowing a higher data rate and bandwidth efficiency, while at the same time requiring better SINR at the receiver for error-free demodulation. Similarly a high code rate will reduce redundancy at the cost of lower error correction capability. Whereas effective adaptation of the MIMO transceiver allows better use of the system's resources.

This work presents a simulation model for this process and gives a clear understanding of the Link Adaptation scheduling, focussing on digital signal processing in the physical layer of the Radio Access networks.

The first chapter presents the tools and protocols needed to model the Physical layer of the LTE standard and the different enabling technologies. The second chapter goes more in details over the Link Adaptation channel stats and gives an insight of how the adaptation is performed with respect to each channel stat signal CQI, PMI and RI. The last one will be a simulation model for the different scheduling techniques using MATLAB. The results will be presented and the discussions will lead to the conclusion of this work

## 1.1 LTE Network Architecture

The high-level network architecture of LTE is comprised of the following three main components:

- The User Equipment UE.
- The Evolved UMTS Terrestrial Radio Access Network E − UTRAN.
- The Evolved Packet Core EPC.

The evolved packet core communicates with packet data networks in the outside world such as the internet, privet corporate networks or the IP multimedia subsystem. The interfaces between the different parts of the system are denoted Uu, S1 and SGi as shown below:

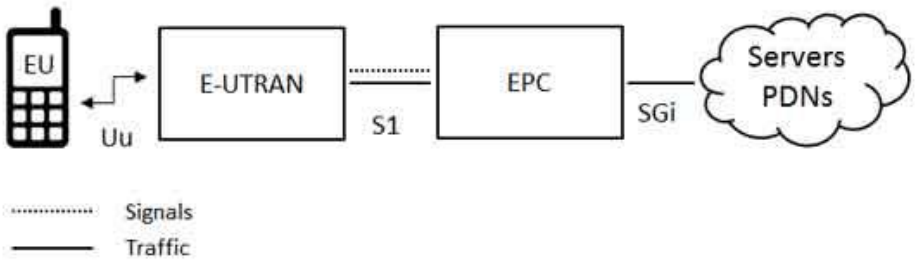


**Figure 1. 1: The interfaces between the differe²nt parts of the system.**

### ➢ The E-UTRAN The access network

The E-UTRAN handles the radio communications between the mobile and the evolved packet core and just has one component, the evolved base stations, called eNodeB.

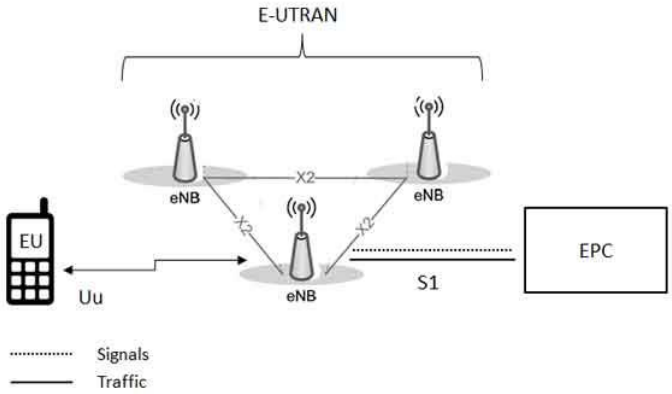


**Figure 1. 2: The architecture of the E−UTRAN.**

The eNodeB supports two main functions:

- It sends and receives radio transmissions for all the mobiles using the analogue and digital signal processing functions of the LTE air interface.
- It controls the low-level operation of all its mobiles, by sending them signaling messages such as handover commands.

### 1.1.1 Frequency bands

LTE supports both FDD and TDD modes, with frequency bands specified as paired and unpaired spectra, respectively. FDD frequency bands are paired, which enables simultaneous transmission on two frequencies: one for the downlink and one for the uplink. The paired bands are also specified with sufficient separations for improved receiver performance. The frequency spectra in LTE are formed as concatenations of resource blocks consisting as shown in table 1.2

**Table1. 2: Channel bandwidth specified in lte.**

| Channel Bandwidth (Mhz) | Number of resource blocks |
|---|---|
| 1.4 | 6 |
| 3 | 15 |
| 5 | 25 |
| 10 | 50 |
| 15 | 75 |
| 20 | 100 |

### 1.1.2 Time framing

In the time domain, LTE organizes the transmission as a sequence of radio frames of length 10 ms, each frame is then subdivided into 10 subframes of length 1 ms.

Each subframe is composed of two slots of length 0.5 ms each. Finally, each slot consists of a number of OFDM symbols, either seven or six depending on whether a normal or an extended cyclic prefix is used. The time-domain structure of the LTE is illustrated in Figure1.3

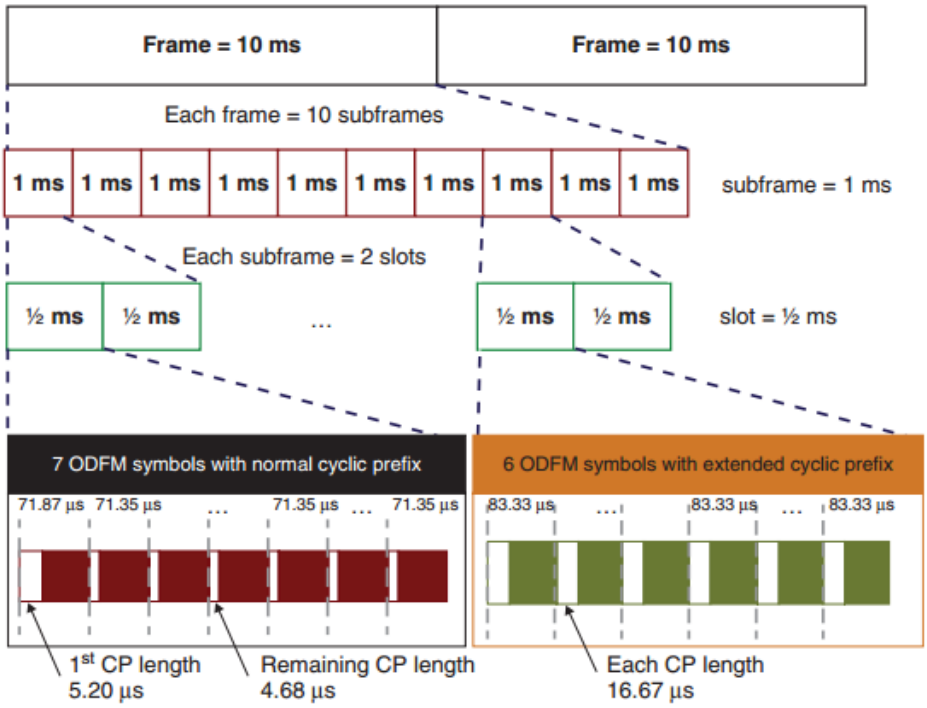


**Figure 1. 3: LTE time domain structure.**

### 1.1.3 Time–Frequency Representation

One of the most attractive features of OFDM is that it maps explicitly to a time–frequency representation for the transmitted signal. After coding and modulation, the physical resource element is mapped onto a time-frequency coordinate system, the resource grid. The resource grid has time on the x-axis and frequency on the y-axis. The x-coordinate of a resource element indicates the OFDM symbol to which it belongs in time. The y-coordinate signifies the OFDM subcarrier to which it belongs in frequency.

### 1.1.4 Resource grid content

Figure 1.4 illustrates the LTE downlink resource grid. A resource element is placed at the intersection of an OFDM symbol and a subcarrier. A resource block is defined as a group of resource elements corresponding to 12 subcarriers or 180 kHz in the frequency domain and one 0.5 ms slot in the time domain. In the case of a normal cyclic prefix with seven OFDM symbols per slot, each resource block consists of 84 resource elements. In the case of an extended cyclic prefix with six OFDM symbols per slot, the resource block contains 72 resource elements. The resource element is the smallest unit of transmission that is subject to frequency-domain scheduling.

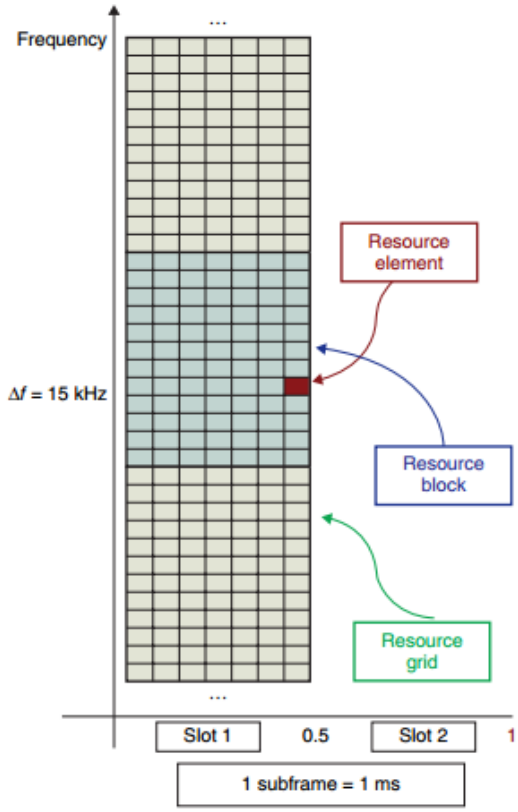


**Figure 1. 4: Resource elements, blocks and grid.**

The LTE transmission scheme provides a time resolution of 12 or 14 OFDM symbols for each subframe of 1 ms, depending on the length of the OFDM cyclic prefix. The number of resource blocks is ranging from 6 to 100, depending on the bandwidth, each containing 12 subcarriers with 15 kHz spacing.

There are essentially three types of information contained in the physical resource grid. Each resource element contains the modulated symbol of either user data or a reference or synchronization signal or control information originating from various higher-layer channels as shown in Figure 1.5. These signals are used for such purposes as channel estimation, channel measurement, and synchronization.

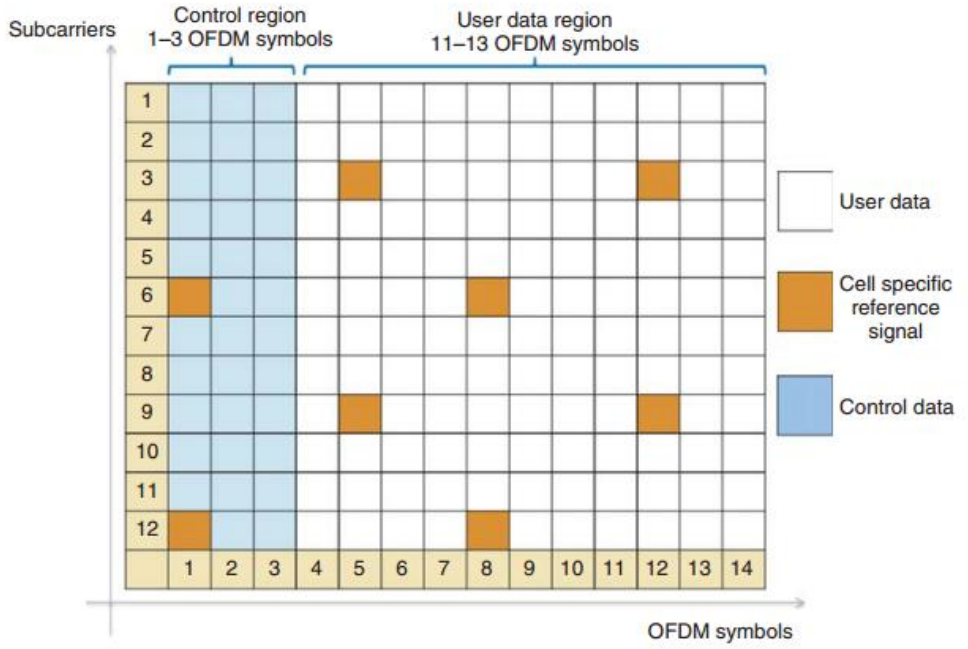


**Figure 1. 5: Physical channel and signal content of LTE downlink subframe in unicast mode.**

## 1.1.5 Physical Channels and Physical Signals

The physical layer comprises physical channels and physical signals. The physical channels are physical resources that carry data or information from the MAC layer. The physical signals are also physical resources that supports the functions of the physical layer, but do not carry any information from the MAC layer. In order that the data can be transported across the LTE radio interface, various channels are used. Figure 1.6 shows the protocol stack of the radio access network and its layer architecture.

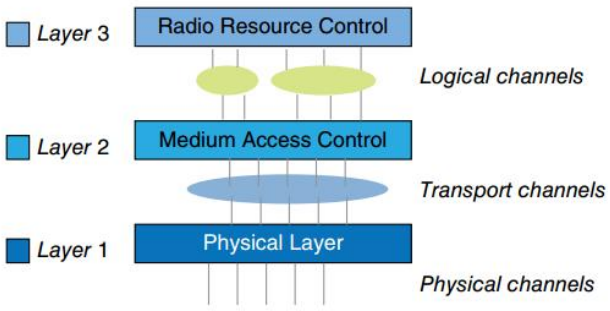


**Figure 1. 6: Layer architecture in a LTE radio access network.**

There are three categories into which the various data channels may be grouped.

**Logical channels:** Provide services for the Medium Access Control (MAC) layer.

**Transport channels:** The physical layer transport channels offer information transfer to Medium Access Control (MAC) and higher layers.

**Physical channel:** These are transmission channels that carry user data and control messages and are ones studied through this work.

The LTE physical channels vary between the uplink and the downlink as each has different requirements and operates in a different manner.

#### 1.1.5.1 Downlink Physical channels

Table 1.3 summarizes the LTE downlink physical channels and there functions.

**Table1. 3: LTE downlink physical channels.**

| Downlink physical channel | Function |
|---|---|
| Physical Downlink Shared Channel (PDSCH) | Unicast user data traffic and paging information |
| Physical Downlink Control Channel(PDCCH) | Downlink Control Information (DCI) |
| Physical Hybrid-ARQ Indicator Channel (PHICH) | HARQ Indicator (HI) and ACK/NACKs for the uplink packets |
| Physical Control Format Indicator Channel (PCFICH) | Control Format Information (CFI) containing information necessary to decode PDCCH information |
| Physical Multicast Channel (PMCH) | Multimedia Broadcast Single-Frequency Network (MBSFN) operation |
| Physical Broadcast Channel (PBCH) | System information required by the terminal in order to access the network during cell search |

Figure 1.7 illustrates the relationship between various logical, transport, and physical channels in LTE downlink architecture for the unicast mode.

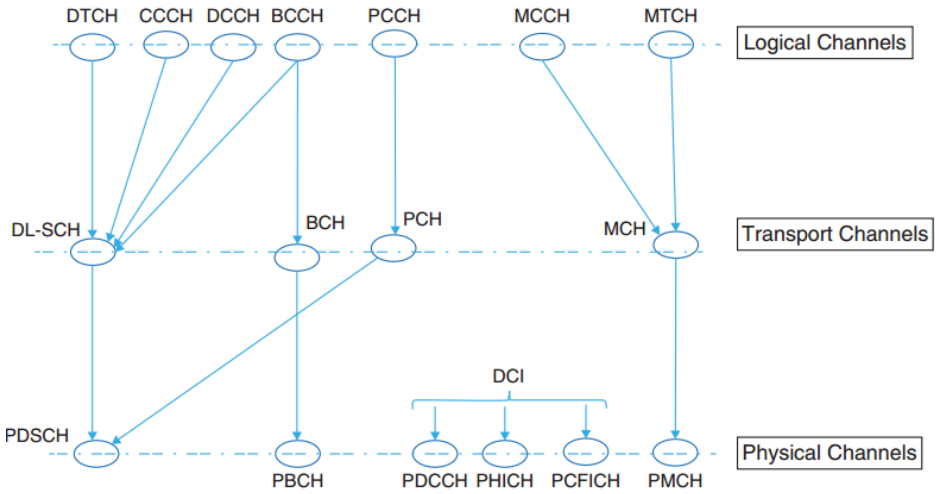


**Figure 1. 7: Mapping LTE downlink logical, transport, and physical channel.**

### 1.1.5.2 Uplink Physical channels

Table 1.4 summarizes the LTE uplink physical channels and their different functions.

**Table1. 4: LTE uplink physical channels.**

| Uplink Physical Channels | Function |
|---|---|
| Physical Uplink Shared Channel (PUSCH) | Uplink user data traffic |
| Physical Uplink Control Channel (PUCCH) | Uplink Control Information (UCI) |
| Physical Random Access Channel (PRACH) | Initial access to network through random access preambles |

Figure 1.8 illustrates the relationship between various logical, transport, and physical channels in LTE uplink architecture for the unicast mode.

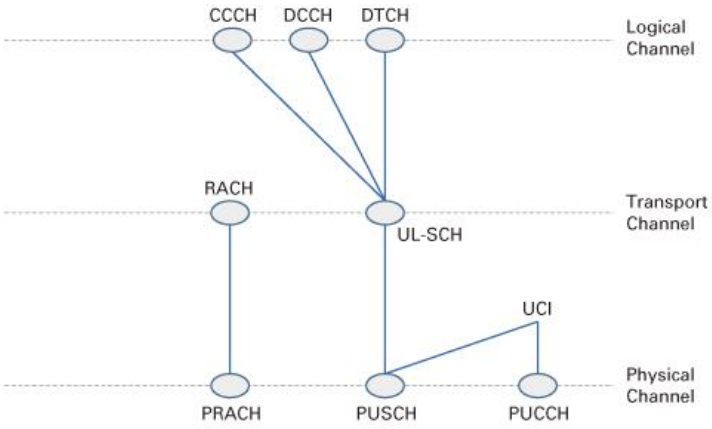


**Figure 1. 8: Mapping LTE uplink logical, transport, and physical channels**

## 1.2 LTE enabling technologies

### 1.2.1 OFDM

The basic concept of OFDM is to send samples concurrently using multiple orthogonal sub-channels rather than sending a sample signal using the entire bandwidth. Because of their orthogonality to each other, the sub-carriers will not interfere on one another. OFDM system can maximize spectral efficiencies and reduce the intersymbole interference (ISI).

The cyclic prefix (CP) is introduced into the OFDM system. It consist on a repetition of the last samples of the data portion that is appended at the beginning of the data payload. As long as the CP duration is longer than the channel delay spread the ISI will be completely eliminated.

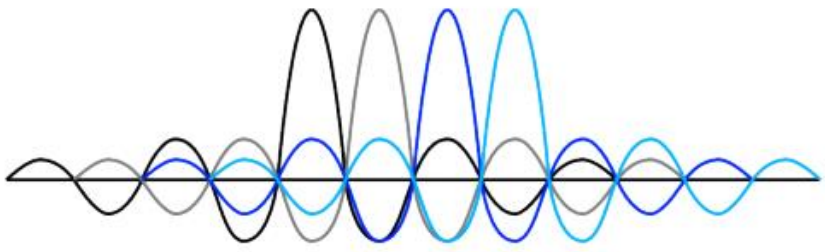

**Figure 1. 9: The spectrum of multiple truncated modulated OFDM subcarriers with constant amplitude.**

### 1.2.1.1 Downlink: Orthogonal Frequency Division Multiple Access (OFDMA)

In OFDMA the channel is divided into many narrow subchannels and transmitted in parallel. The main advantage in OFDMA is its ability to allocate subcarriers dynamically in time and frequency, allowing more users to access the network as seen in figure 1.10.

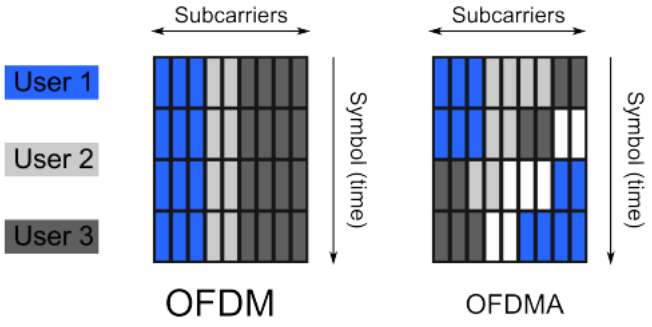


**Figure 1. 10 : Subcarrier allocation in OFDM and OFDMA.**

### 1.2.1.2 Uplink: Single-Carrier Frequency Division Multiple Access (SCFDMA)

By using the time domain data signals and transform it to frequency domain by a DFT before passing through OFDMA modulation. This techniques reduce the instantaneous transmit power implying increase power-amplifier efficiency, low-complexity and flexible bandwidth assignment. Using SC-FDMA allows the usage of a single carrier transmission system. In Figure 1.11 on the next page a graphical comparison of OFDMA and SC-FDMA are shown.

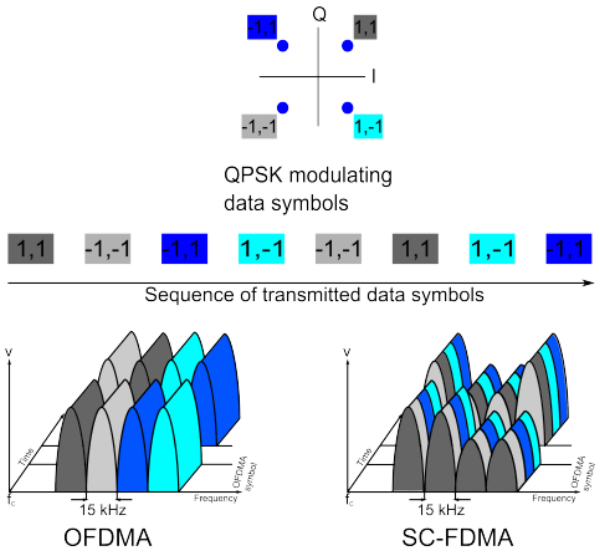


**Figure 1. 11 : Transmission of a series of QPSK symbols in both OFDMA and SC-FDMA.**

### 1.2.1.3 OFDM Transmitter Chain

Figure 1.12 is a block diagram of the LTE OFDM signal chain used by the LTE base stations for OFDM symbol transmission. The transmission chain is composed of several blocks that takes a set of bits produced by higher layers and converts the bits to OFDM symbols for transmission over the wireless channel.

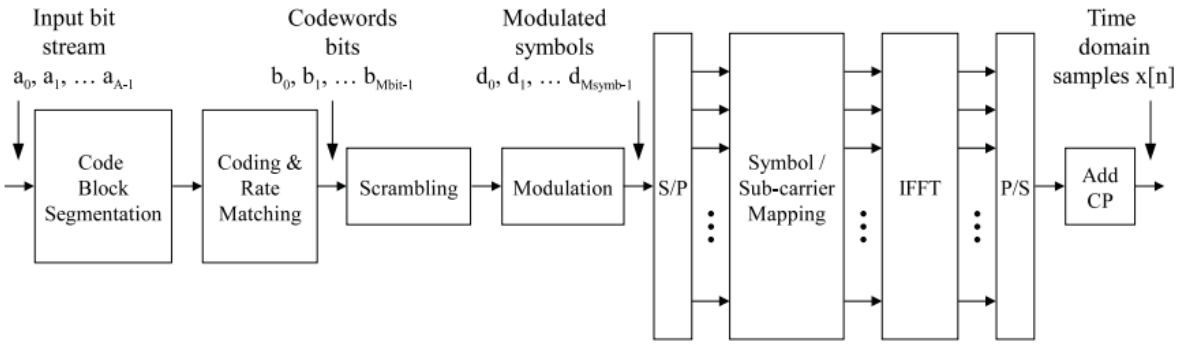


**Figure 1. 12: LTE OFDM Transmitter Chain with Modulation and Coding, IFFT and CP**

The first step in the process of OFDM symbol generation is code block segmentation. The bit stream is separated into blocks of bits and cyclic redundancy check (CRC) parity bits are attached to the blocks for error detection. Forward error correction is made possible by the coding and rate matching blocks using the LTE turbo encoder, which helps to overcome the errors introduced by the channel using interleaving and convolutional encoding. At the receiver the redundant information is used by the iterative turbo decoder to recover the original codewords and messages transmited by the base station. After channel coding, the bits are scrambled with identification numbers and then modulated onto sub-carriers and mapped across the frequency domain of the channel. The inverse fast Fourier transform (IFFT) is used to obtain the OFDM symbol in the time domain.

## 1.2.2 Channel Coding

Channel coding is one of the most important aspects in digital communication systems, which can be considered as the main difference between analogue and digital systems making error detection and correction possible. Channel coding is utilized In order to correct bit errors, introduced by channel variations and noise. Error correction exists in two main forms: ARQ (Automatic Repeat Request) and FEC (Forward Error Correction). With ARQ the receiver requests retransmission of data packets, if errors are detected, using some error detection mechanism. In FEC some redundancy bits are added to the data bits, which is done

either blockwise (so-called block coding) or convolutional. LTE both block codes and convolutional codes are used. There is also an enhanced coding technique used in LTE, called Turbo code, which has performances within a few tenth of a dB from the Shannons limit.

In the LTE standard, turbo coding is the only channel coding mechanism used to process the user data. The turbo encoder is built with two rate where the encoders are based on 1/3 RSC (Recursive Systematic Convolutional) codes, shown in figure 1.13, and their generator polynomial is given by G= [1, $g_0/g_1$] where $g_0$ = [1011] (feedback) and $g_1$ = [1101] (feed forward).

The RSC encoders operate on the input bits stream and the interleaved bit stream producing two parity bits for each bit input into the turbo encoder. The concatenated systematic and parity bits produce a fixed rate bit sequence based on the sequence of input bits, known as the mother code. The mother code is then adapted to match the available physical layer resources by puncturing or repeating the mother code to achieve the desired code rate. The amount of physical layer resources (bits) available are determined by the UE's modulation and coding scheme (MCS) selection.

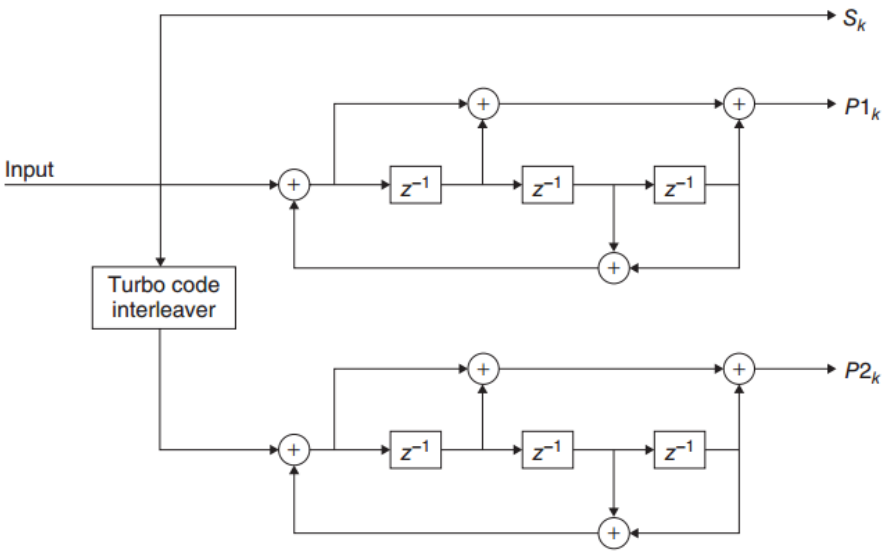


**Figure 1. 13: Block Diagram of the LTE Turbo Encoder.**

### 1.2.3 MIMO

MIMO system employs multiple antennas at both transmitter and receiver. The idea behind it is that the signals on the transmit antennas at one end and the received antennas at the other ends are combined in such a way that the quality of the communication for each MIMO user will be improved [4]. The improved quality can be quantified in terms of error rate or throughput (data rate) depending on how MIMO combines the signals.

A key feature for MIMO is its ability to turn multipath propagation, traditionally a problem in wireless communication, into a benefit for the user. MIMO effectively takes the advantages of random fading [4] [5]. In the presence of random fading, the probability of losing the signal decrease with the number of decorrelated antenna elements being used [3]. Thus, in MIMO, the spatial correlation between antenna elements is the parameter that determines the performance. This spatial correlation determines the independency between antenna elements and thus the amount of spatial diversity that can be exploited.

#### 1.2.3.1 MIMO Channel

##### 1.2.3.1.1 Flat fading

A transmitted signal undergoes flat fading when the signal bandwidth (BW) is less than the channel coherence bandwidth. In flat fading, through the spectrum of the transmitted signal is preserved, the received signal varies in amplitude and encounters deep fades of 20 to 30 dB.

##### 1.2.3.1.2 Frequency selective

For Frequency selective fading or wide band channel, the signal bandwidth is greater than the channel coherence bandwidth. In frequency selective fading, time dispersion causes inters-symbol interference at the receiver making the multiple versions of the received signal attenuated and delayed in time to a different degrees.

##### 1.2.3.1.3 LTE specific channels

There are three different multipath fading channels for LTE which are pecific channels made by the Third Generation Partnership Project (3GPP) namely:

- The Extended Pedestrian A (EPA)
- The Extended Vehicular A (EVA)

- The Extended Typical Urban (ETU)

These models enable us to evaluate the performance of the transceiver in various reference channel conditions. In this work the EVA channel has been considered.

### 1.2.3.2 MIMO Receiver

The receiver uses an equalizer to produce the best estimate of the transmitted symbols. In LTE, equalization is accomplished in the frequency domain. Channel estimation and equalization are accomplished by inserting known reference signals in the frequency domain to estimate the channel and the channel effect can then be removed.

Three algorithms are considered:

- Zero Forcing (ZF) equalizer
- Minimum Mean Square Error (MMSE) equalizer
- Sphere Decoder (SD) equalizer

#### 1.2.3.2.1 ZF equalizer

The ZF receiver inverses the MIMO channel matrix. The major drawback of the ZF receiver is noise enhancement. Although the ZF receiver eliminates the interference, performance becomes poor when the channel of the signal of interest is almost collinear to the interference subspace, or in other words when the channel matrix is almost rank deficient. [6]

#### 1.2.3.2.2 MMSE equalizer

The MMSE receiver minimises the average estimation error on the transmitted symbols. The average is taken over the transmitted symbols and the noise [6]. The mean square error (MSE) can be illustrated by equation 1

$$\mathbf{Ex, n} = \|\widehat{\boldsymbol{X}} - \boldsymbol{X}\|^{\mathbf{2}} \qquad (1)$$

Where $\widehat{\boldsymbol{X}}$ is the estimated symbol and $\boldsymbol{X}$ is the transmitted symbol. The ZF receiver also minimises the output MSE but under the constraint of complete inter symbol interference (ISI) elimination.

#### 1.2.3.2.3 Sphere decoding equalizer

The Sphere Decoding (SD) receiver finds the transmitted signal vector with minimum maximum likelihood (ML) metric, that is, to find the ML solution vector. However it considers only a small set of vectors within a given sphere rather than all possible transmitted signal vectors. SD adjusts the sphere radius until there exists a single vector (ML solution vector) within a sphere. It increases the radius when there exists no vector within a sphere, and decreases the radius when there exists multiple vectors within the sphere. [6]

### 1.2.3.3 Transmission modes in LTE downlink

#### 1.2.3.3.1 Mode 1 (SIMO)

There is a single transmit antenna and multiple receiver antennas. Thus Mode 1 of LTE has only one transmit antenna.

#### 1.2.3.3.2 Mode 2 (transmit diversity)

Transmit diversity, sends the same data via various antennas. As Each antenna stream is using different frequency resources and different coding. It provides a stronger transmission and improves the SNR. Transmit diversity is used as a fall-back option in LTE for some transmission modes.

#### 1.2.3.3.3 Mode 3 (open-loop spatial multiplexing)

Is employed for high-mobility scenarios and consists **o**f applying either transmit diversity or fixed (non-adaptive) precoding. Switching between these alternatives is performed by means of rank adaptation (i.e., transmit diversity for rank 1 and spatial multiplexing with fixed precoding for rank 2). This operation mode allows for increasing throughput of high-mobility users experiencing good channel conditions.

#### 1.2.3.3.4 Mode 4 (closed-loop spatial multiplexing)

Implies adaptive precoding and rank adaptation (1, 2, 3, or 4) based on the UE reports. A rank 1 transmission corresponds to beam forming, whereas a rank 2, 3, or 4 is associated with spatial multiplexing configuration. The UE reports must be reliable for a proper adaptation process; therefore, this mode is only suitable for users moving at low or medium speed.

### 1.2.4 Link Adaptation

The Link Adaption (LA) refers to the techniques deployed to adapt the transmission parameters to the time varying nature of the radio link. The transmission parameters include, for example, the Modulation and Coding Schems (MCS), the transmit power level, the transmission bandwidth. The spectral efficiency can for example be improved by using a more robust MCS under adverse channel conditions and vice versa when the channel conditions improve.

## 1.3 Physical Layer Processing

Physical layer (PHY) modelling involves all the processing performed on bits of data that are handed down from the higher layers to the PHY. It describes how various transport channels are mapped to physical channels, how signal processing is performed on each of these channels, and how data are ultimately transported to the antenna for transmission.

### 1.3.1 Downlink Processing

The chain of signal processing operations performed in the transmitter can be summarized as the combination of transport block processing and physical channel processing. The processing stack is completely specified in 3GPP documents describing the multiplexing and channel coding [7] and physical channels and modulation [4]. The baseband signal processing chain applied to the combination of DLSCH and PDSCH can be summarized as follows:

- Transport-block CRC (Cyclic Redundancy Check) attachment
- Code-block segmentation and code-block CRC attachment
- Turbo coding based on a one-third rate
- Rate matching to handle any requested coding rates
- Code-block concatenation to generate codewords
- Scrambling of coded bits in each of the codewords to be transmitted on a physical channel
- Modulation of scrambled bits to generate complex-valued modulation symbols
- Mapping of the complex-valued modulation symbols on to one or several transmission layers

- Precoding of the complex-valued modulation symbols on each layer for transmission on the antenna ports
- Mapping of complex-valued modulation symbols for each antenna port to resource elements
- Generation of complex-valued time-domain OFDM signal for each antenna port.

Figure1.14 illustrates the combination of the signal processing applied to transport blocks delivered to the PHY from the MAC layer until the OFDM signal is transferred to antennas for transmission.

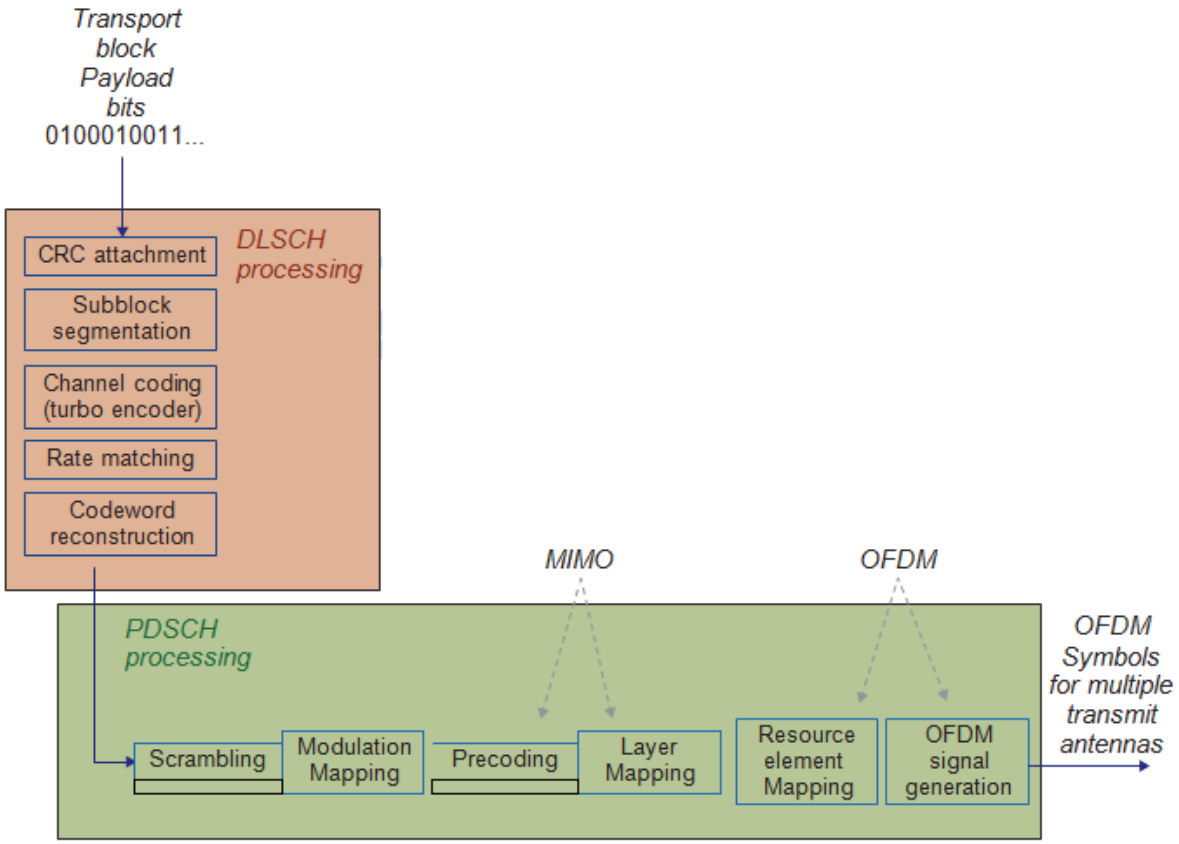


**Figure 1. 14 : Signal processing chain of downlink DLSCH and PDSCH.**

## Conclusion

In this chapter we have studied the physical layer specifications of the LTE standards, which are highly important to understand the link adaptation mechanism. First, we examined the air interface of the standard, detailing its frequency bands, bandwidths, time framing, and time–frequency structure. We then elaborated on the multicarrier schemes of the standard: OFDM for downlink transmission and SC-FDM for uplink transmission. We identified the constituents of the OFDM resource grid.

We then covered the physical channels and physical signals used in both uplink and downlink transmissions. We also provided an introduction to the MIMO schemes used in the standard, which completely specify various transmission modes. Finally, we summarized the sequence of operations performed in downlink and uplink transmissions.

## Introduction

Link adaptation is defined as a collection of techniques for changing and adapting the transmission parameters of a mobile communication system to better respond to the dynamic nature of the communication channel. Depending on the channel quality, we can use different modulation and coding techniques (adaptive modulation and coding), change the number of transmit or receive antennas (adaptive MIMO), and even change the transmission bandwidth (adaptive bandwidth) Typically, we need to either minimize the amount of resources allocated to each user or match the resources to the type and priority of the user data. Channel-dependent scheduling aims to accommodate as many users as possible, while satisfying the best quality-of-service requirements that may exist based on the instantaneous channel condition. [8]

The cost associated with this adaptation is the additional computational complexity involved in implementing link-aware schedulers.

## 2.1 System Model

Link adaptation is all about adapting to the channel conditions and changing system parameters based on actual channel quality. The LTE standard enables link adaptations that can help us make use of the spectrum more efficiently. The cost associated with this adaptation is the additional computational complexity involved in implementing link-aware schedulers.

Figure 2.1 illustrates the typical operations involved in link adaptation, which are subdivided into downlink and uplink operations.

The series of operations performed in a typical link adaptation scenario can be summarized as follows:

1. At subframe (n), the downlink transmitter forms the resource grid from the user data PDSCH, and the Downlink Control Information, DCI (the PDCCH). The DCI contains the scheduling assignments that help the mobile receiver correctly decode the subframe information. The information contained in the PDCCH includes the MCSs, the precoder matrix, rank information, and the MIMO mode used.

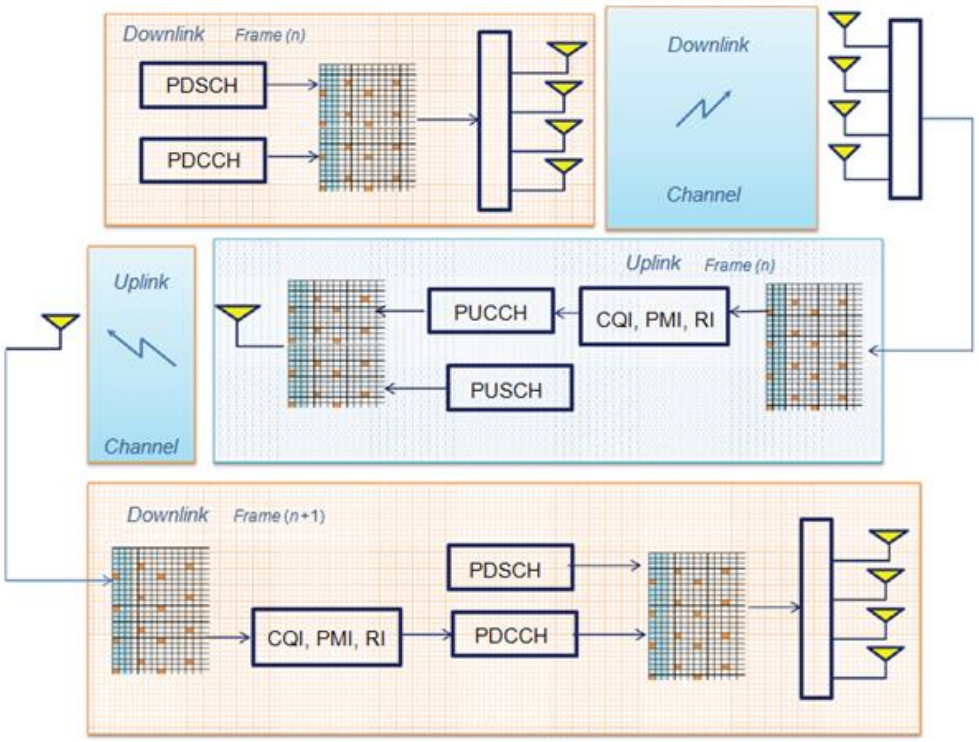


**Figure 2. 1 : Sequence of downlink and uplink operations involved in link adaptation.**

2. The mobile receiver decodes the received resource grid. It estimates the received channel matrix and performs measurements of the CQI, the PMI, and the RI.
3. As part of uplink transmission, the UE embed the channel quality measures within the PUCCH and transmit to the base station (eNodeB) as a closed-loop feedback mechanism.
4. The base station (eNodeB) receiver decode the PUCCH information to obtain channel measurements. This enables the system scheduler to decide whether or not to adapt various system parameters in the next frame.

At the base station (eNodeB) in the downlink transmitter operations for the next sub-frame ($n$ + 1), the scheduling decisions based on channel conditions are encoded into the PDCCH information and transmitted to the mobile. These include the new MCSs, precoder matrix, rank information, and MIMO mode that are now adapted based on the actual channel quality in the last subframe ($n$). This full feedback process is then repeated for each subframe. [8]

## 2.2 Channel-state report for Link Adaptation

At the mobile receiver, three types of channel-state report are generated and transmitted to the base station:

### 2.2.1 Channel Quality Indicator

The CQI report gives a measure of the mobile radio channel quality. It provides a recommendation concerning the best MCS for the communication. The CQI estimation is performed in two steps:

1. SINR estimation: The SINR measure is computed as a function of the decoded bits in the receiver and the MIMO receiver output.
2. Spectral efficiency lookup: The computed SINR values are mapped to a spectral efficiency measure defined as the product of the number of modulated bits per symbol and the coding rate. For each SINR measure, distinct modulation schemes and coding rates are found through a table lookup.

Let us define $\boldsymbol{G}$ as the optimum equalizer that transforms the received signal **Y (n)** into the equalized signal **X (n)** as the best linear estimate of the transmitted signal **X (n).** The error signal **e (n)** is then expressed in equation 2.

$$\boldsymbol{e(n) = \widehat{X}(n) - X(n) = GY(n) - X(n)} \qquad (2)$$

For the CQI estimation, a very simplified approximation of the SINR measure is computed, defined by equation 3, as the ratio of the transmitted signal power $\boldsymbol{\sigma^2 x}$ to the error signal power $\boldsymbol{\sigma^2 e}$.

$$\boldsymbol{SINR = 10\ \log_{10}\left(\frac{\sigma_x^2}{\sigma_e^2}\right)} \qquad (3)$$

The terminal reports the measured CQI to the eNodeB by mapping the measured SNR according to Figure 2.2. In the LTE simulator, the mapping of the SNR to the CQI for a BLER of 0.1 is approximated through a linear function as shown in the figure.

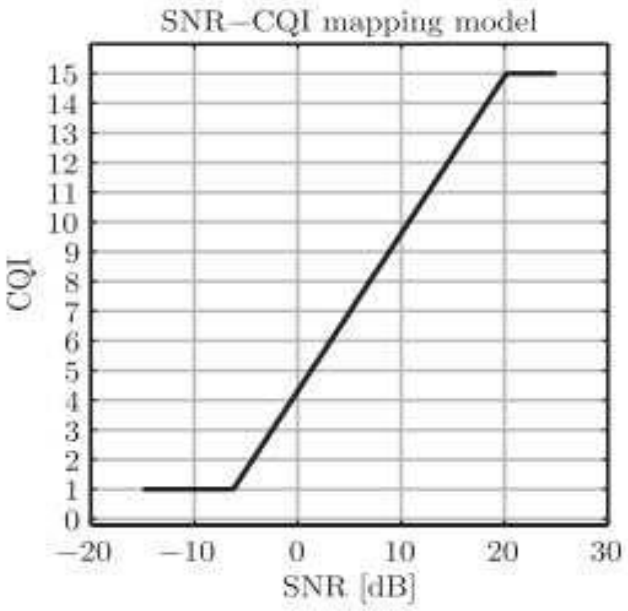


**Figure 2. 2: SNR-CQI mapping model.**

In order to update the modulation scheme (Ms) and the coding rate (Cr) outputs, a table lookup operation with the CQI index is performed (see Table 2.1).

For the first seven values of the CQI index (indices 0–6), a mapping to a QPSK modulation with a modulation rate of 2 bits per symbol is done. The next three CQI indices (7, 8, and 9) are mapped to the 16QAM modulator with a modulation rate of 4 bits per symbol.Finally, the last six CQI indices (10–15) are mapped to 64QAM with a 6-bitsper-symbol modulation rate.

Technically, the CQI index 0 signals an out-of-range message and does not participate in modulation mapping. For simplicity, this index is included in the MATLAB function with the QPSK set. The 16 mapping values for the coding-rate (Cr) mapping of spectral efficiency measures to modulation and coding rates are specified by the LTE standard document [9]. The combined information is provided in Table 2.1.

**Table2. 1: Lookup table for mapping SINR estimate to modulation scheme and coding rate.**

| CQI index | Modulation | Coding Rate | Spectral Efficiency (bps/Hz) | SINR Estimate (dB) |
|---|---|---|---|---|
| **1** | QPSK | 0.0762 | 0.1523 | -6.7 |
| **2** | QPSK | 0.1172 | 0.2344 | -4.7 |
| **3** | QPSK | 0.1885 | 0.3770 | -2.3 |
| **4** | QPSK | 0.3008 | 0.6016 | 0.2 |
| **5** | QPSK | 0.4385 | 0.8770 | 2.4 |
| **6** | QPSK | 0.5879 | 1.1758 | 4.3 |
| **7** | 16QAM | 0.3691 | 1.4766 | 5.9 |
| **8** | 16QAM | 0.4785 | 1.9141 | 8.1 |
| **9** | 16QAM | 0.6016 | 2.4063 | 10.3 |
| **10** | 64QAM | 0.4551 | 2.7305 | 11.7 |
| **11** | 64QAM | 0.5537 | 3.3223 | 14.1 |
| **12** | 64QAM | 0.6504 | 3.9023 | 16.3 |
| **13** | 64QAM | 0.7539 | 4.5234 | 18.7 |
| **14** | 64QAM | 0.8525 | 5.1152 | 21.0 |
| **15** | 64QAM | 0.9258 | 5.5547 | 22.7 |

The higher the value of the CQI measure, the higher the modulation order and the coding rate. There are two types of CQI report, based on their granularity: a wideband CQI report assigns a single MCS value for the whole system bandwidth, while a subband CQI report assigns multiple MCS values to different contiguous resource blocks. Through all this work a wideband CQI reporting is used [10].

### 2.2.2 Precoding Matrix Estimation:

Precoding is based on transmit beamforming concepts with the provision of allowing multiple beams to be simultaneously transmitted in the MIMO system. The LTE specification defines a set of complex weighting matrices for combining the layers before transmission using up to 4 by 4 MIMO tranceiver antenna configurations [13]. For a 2 by 2 MIMO

tranceiver configuration, the weighting matrix, $W$ is multiplied by the input layers, equation 4, to generate the precoded signals to be transmitted .

$$\begin{bmatrix} y^{(0)}(i) \\ y^{(1)}(i) \end{bmatrix} = w(i) \begin{bmatrix} x^{(0)}(i) \\ x^{(1)}(i) \end{bmatrix} \qquad (4)$$

Here, $x^{(q)}(i)$ are the input layers prior to precoding ($q$ = 0, 1) and $y^{(q)}(i)$ are the precoded signals applied to each transmit antenna. The simplest precoding matrix maps each layer to a single antenna dedicated to transmitting that layer, without any coupling to other antennas. In this case, the weighting matrix in equation 4, defined with codebook index 0, becomes:

$$w(i) = \frac{1}{\sqrt{2}} \begin{bmatrix} 1 & 0 \\ 0 & 1 \end{bmatrix} \qquad (5)$$

Resulting in the following transmitted data asshown in equation 6 and 7.

$$y^{(0)}(i) = \frac{1}{\sqrt{2}} x^{(0)}(i) \qquad (6)$$

$$y^{(1)}(i) = \frac{1}{\sqrt{2}} x^{(1)}(i) \qquad (7)$$

A second precoding matrix, defined with codebook index 1, equation 8, provides a linear combination of the sums and differences of the two input layers respectively.

$$w(i) = \frac{1}{2} \begin{bmatrix} 1 & 1 \\ 1 & -1 \end{bmatrix} \qquad (8)$$

Resulting in the following transmitted data shown in equation 9 and 10.

$$y^{(0)}(i) = \frac{1}{2} x^{(0)}(i) + \frac{1}{2} x^{(1)}(i) \qquad (9)$$

$$y^{(1)}(i) = \frac{1}{2} x^{(0)}(i) - \frac{1}{2} x^{(1)}(i) \qquad (10)$$

This codebook selection allows a portion of each signal layer to be transmitted through each antenna Figure.3, and depending on the channel conditions, providing some flexibility when attempting to improve and equalize the SINR at each MIMO receiver.

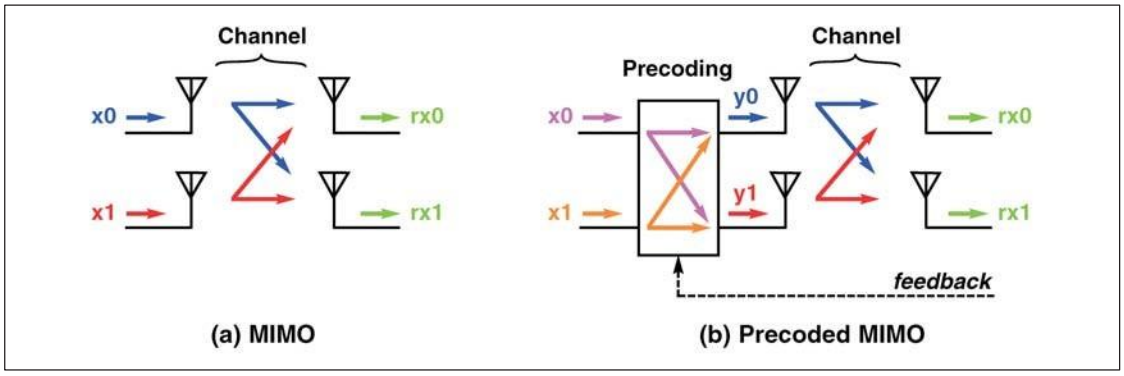


**Figure 2. 3: Block diagram of (a) MIMO without precoding and (b) MIMO with precoding.**

The LTE specification for precoding spatially multiplexed transmissions includes a total of four codebook matrices for two transmit antenna configurations (Table2.2) and 16 codebook matrices for four transmit antenna systems (Table2.3). Proper selection of the optimal precoding matrix requires knowledge of the current channel conditions at the transmitter. The channel conditions are provided through feedback from the MIMO receiver creating a closed-loop system. For an LTE precoded downlink transmission, the mobile terminal or user equipment (UE) will measure the channel characteristics and determine the precoding matrix index (PMI), this information will be sent to the base station (eNodeB) which would modify the precoding codebook selection to improve overall system performance. [11]

**Table2. 2: Precoding matrices for two transmit antennas in LTE spatial multiplexing.**

| **Coode book index** | **Number of layers V** | |
|---|---|---|
| | **1** | **2** |
| 0 | $\frac{1}{\sqrt{2}}\begin{bmatrix}1\\1\end{bmatrix}$ | $\frac{1}{\sqrt{2}}\begin{bmatrix}1 & 0\\0 & 1\end{bmatrix}$ |
| 1 | $\frac{1}{\sqrt{2}}\begin{bmatrix}1\\-1\end{bmatrix}$ | $\frac{1}{\sqrt{2}}\begin{bmatrix}1 & 1\\1 & -1\end{bmatrix}$ |
| 2 | $\frac{1}{\sqrt{2}}\begin{bmatrix}1\\j\end{bmatrix}$ | $\frac{1}{\sqrt{2}}\begin{bmatrix}1 & 0\\j & -j\end{bmatrix}$ |
| 3 | $\frac{1}{\sqrt{2}}\begin{bmatrix}1\\-j\end{bmatrix}$ | – |

**Table2. 3: Precoding matrices for four transmit antennas in LTE spatial multiplexing.**

| Code book index | $U_n$ | Number of layers $V$ | | | |
|---|---|---|---|---|---|
| | | 1 | 2 | 3 | 4 |
| 0 | $U_0 = [1 \quad -1 \quad -1 \quad -1]^T$ | $W_0^{\{1\}}$ | $W_0^{\{14\}}/\sqrt{2}$ | $W_0^{\{124\}}/\sqrt{3}$ | $W_0^{\{1234\}}/2$ |
| 1 | $U_1 = [1 \quad -j \quad 1 \quad j]^T$ | $W_1^{\{1\}}$ | $W_1^{\{12\}}/\sqrt{2}$ | $W_1^{\{123\}}/\sqrt{3}$ | $W_1^{\{1234\}}/2$ |
| 2 | $U_2 = [1 \quad 1 \quad -1 \quad 1]^T$ | $W_2^{\{1\}}$ | $W_2^{\{12\}}/\sqrt{2}$ | $W_2^{\{123\}}/\sqrt{3}$ | $W_2^{\{3214\}}/2$ |
| 3 | $U_3 = [1 \quad j \quad 1 \quad -j]^T$ | $W_3^{\{1\}}$ | $W_3^{\{12\}}/\sqrt{2}$ | $W_3^{\{123\}}/\sqrt{3}$ | $W_3^{\{3214\}}/2$ |
| 4 | $U_4 = \left[1 \quad (-1-j)/\sqrt{2} \quad -j \quad (1-j)/\sqrt{2}\right]^T$ | $W_4^{\{1\}}$ | $W_4^{\{14\}}/\sqrt{2}$ | $W_4^{\{124\}}/\sqrt{3}$ | $W_4^{\{3214\}}/2$ |
| 5 | $U_5 = \left[1 \quad (1-j)/\sqrt{2} \quad j \quad (-1-j)/\sqrt{2}\right]^T$ | $W_5^{\{1\}}$ | $W_5^{\{14\}}/\sqrt{2}$ | $W_5^{\{124\}}/\sqrt{3}$ | $W_5^{\{1234\}}/2$ |
| 6 | $U_6 = \left[1 \quad (1+j)/\sqrt{2} \quad -j \quad (-1+j)/\sqrt{2}\right]^T$ | $W_6^{\{1\}}$ | $W_6^{\{13\}}/\sqrt{2}$ | $W_6^{\{134\}}/\sqrt{3}$ | $W_6^{\{1324\}}/2$ |
| 7 | $U_7 = \left[1 \quad (-1+j)/\sqrt{2} \quad j \quad (1+j)/\sqrt{2}\right]^T$ | $W_7^{\{1\}}$ | $W_7^{\{13\}}/\sqrt{2}$ | $W_7^{\{134\}}/\sqrt{3}$ | $W_7^{\{1324\}}/2$ |
| 8 | $U_8 = [1 \quad -1 \quad 1 \quad 1]^T$ | $W_8^{\{1\}}$ | $W_8^{\{12\}}/\sqrt{2}$ | $W_8^{\{124\}}/\sqrt{3}$ | $W_8^{\{1234\}}/2$ |
| 9 | $U_9 = [1 \quad -j \quad -1 \quad -1]^T$ | $W_9^{\{1\}}$ | $W_9^{\{14\}}/\sqrt{2}$ | $W_9^{\{134\}}/\sqrt{3}$ | $W_9^{\{1234\}}/2$ |
| 10 | $U_{10} = [1 \quad 1 \quad 1 \quad -1]^T$ | $W_{10}^{\{1\}}$ | $W_{10}^{\{13\}}/\sqrt{2}$ | $W_{10}^{\{123\}}/\sqrt{3}$ | $W_{10}^{\{1324\}}/2$ |
| 11 | $U_{11} = [1 \quad j \quad -1 \quad j]^T$ | $W_{11}^{\{1\}}$ | $W_{10}^{\{13\}}/\sqrt{2}$ | $W_{10}^{\{134\}}/\sqrt{3}$ | $W_{10}^{\{1324\}}/2$ |
| 12 | $U_{12} = [1 \quad -1 \quad -1 \quad 1]^T$ | $W_{12}^{\{1\}}$ | $W_{12}^{\{12\}}/\sqrt{2}$ | $W_{12}^{\{123\}}/\sqrt{3}$ | $W_{12}^{\{1234\}}/2$ |
| 13 | $U_{13} = [1 \quad -1 \quad 1 \quad -1]^T$ | $W_{13}^{\{1\}}$ | $W_{13}^{\{13\}}/\sqrt{2}$ | $W_{13}^{\{123\}}/\sqrt{3}$ | $W_{13}^{\{1324\}}/2$ |
| 14 | $U_{14} = [1 \quad 1 \quad -1 \quad -1]^T$ | $W_{14}^{\{1\}}$ | $W_{14}^{\{13\}}/\sqrt{2}$ | $W_{14}^{\{123\}}/\sqrt{3}$ | $W_{14}^{\{3214\}}/2$ |
| 15 | $U_{15} = [1 \quad 1 \quad 1 \quad 1]^T$ | $W_{15}^{\{1\}}$ | $W_{15}^{\{12\}}/\sqrt{2}$ | $W_{15}^{\{123\}}/\sqrt{3}$ | $W_{15}^{\{1234\}}/2$ |

### 2.2.3 Rank Estimation:

The rank estimation measure (RI) denotes the number of transmission layers or independent data streams for a spatial multiplexing system. The reporting is done as following:

- UE calculates the preferred number of transmitted spatial layers periodically and reports RI to eNodeB.
- Based on the received reporting RI, eNodeB selects the number of transmission spatial layers to transmit the desired signals for UE.

When UE experience bad SNR and it would be difficult to decode transmitted downlink data it gives early warning to eNodeB by stating Rank Indication value as 1. When UE experience good SNR it pass this information to eNodeB by indicating rank value as 2.

By using RI the system could switch the transmission mode between transmit diversity and spatial multiplexing mode. The system will undergo spatial multiplexing transmission if the RI is equal to the transmitting antennas number and transmit diversity mode if the RI is less than it. The antennas number and data rate remained constant while the manipulated parameter will be the threshold that trigger the switching. Thus, a wideband rank value is used for the simulation. RI channel state designated the number of layers that the spatial multiplexing channel can adapt to [10].

## 2.3 Work description:

Various ways of using the Channel-State Information (CSI: CQI, PMI, and RI estimates) to adapt various transceiver parameters in successive subframes are investigated. In the next chapter, what can be regarded as some very simple scheduling scenarios is discussed. These algorithms are meant to provide a framework for the implementation of adaptation algorithms in MATLAB.

Four types of adaptation applied to a single-codeword closed-loop spatial multiplexing system (single-codeword model for LTE transmission mode 4). First an adaptive modulation will be studied, then an adaptive modulation and coding mechanism by using the CQI measure. The third one is a combinition between adaptive modulation and coding with adaptive precoder selection based on the PMI measure. Finally, a combination of adaptive layer mapping using the RI measure and all the previous adaptations will be done.

## Introduction

This chapter presents the results of our simulations for link adaptation techniques. The motivations of the LTE standard for the use of these technique are clarified.

## 3.1 Simulation Model Description

The figure3.1 represents the LTE physical layer model as defined by the standard. This model has been taken as a reference for the implementation of this work using MATLAB. Each block is represented by a MATLAB functional block as shown in figure 3.2.

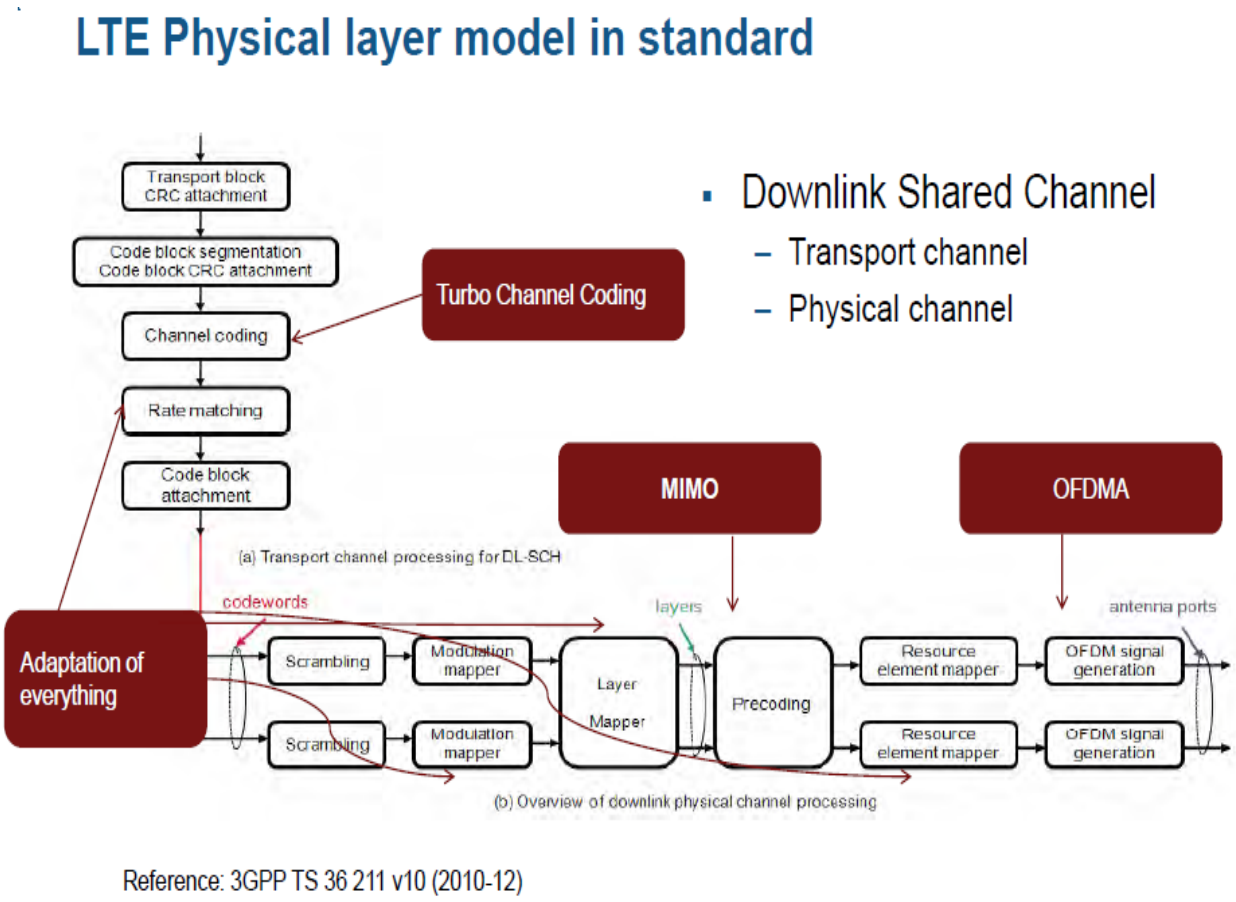


**Figure 3. 1: LTE physical layer model as defined by the standard**

The figure 3.2 shows how each physical layer block has been mapped to the corresponding Matlab function

For each experiment a test bench has been created. Where at first, it sets the relevant experiment parameters found in the MATLAB script commlteMIMO_params. It initializes

three LTE transceiver parameter structures by calling the function commlteMIMO_initialize. Then it sets up while loop to call the main transceiver functions.

Each iteration of the while loop processes one subframe of data. At each subframe, information regarding current modulation scheme (modType parameter), current coding rate (cRate parameter) and their averages are printed in the MATLAB workspace.

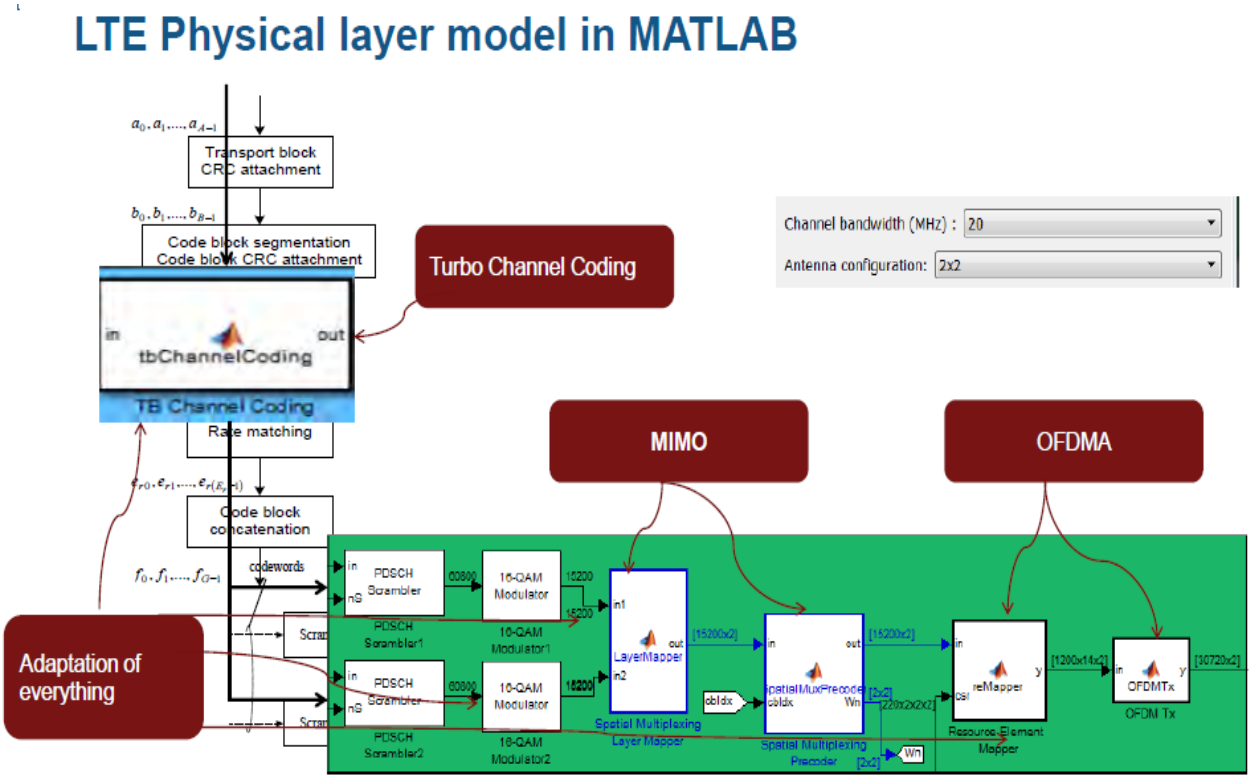


**Figure 3. 2: System model for the LTE physical layer**

By changing parameters such as modulation scheme and coding rate in file commlteMIMO_params you can experiment with various test conditions and initalize modulation and coding rate. By changing the link SNR (the parameter snrdB) you can see the eff ect of AWGN noise on the overall performance.

The transmission mode is always the closed loop spatial multiplexing by setting the parameter txMode initialized as 4. It is also possible to explore a 2x2 or a 4x4 antenna configuration by changing the numTx and numRx parameters respectively

For all the simulations to come the parameters initially set are summarized in a table for each section. Different channel models are available for this model, some of them have been covered in this work.

## 3.2 CQI Based Adaptation

In this section, the CQI channel-state report is considered in order to adaptively change the modulation and coding scheme of the transmission. A wideband adaptation is used which means that at any given subframe all the resource blocks will have the same properties and the adaptation occurs within each subframe.

The CQI adaptation works in two steps as mentioned in the previous chapter, first it estimates the SNIR of the channel then it performs a table look up (Table2.1) to match the estimated SNIR to the suited modulation and coding rate. The value of this measure is computed such that the Bit Error Rate (BER) using the LTE standard recommendation will not exceed 10%.

To understand the design trade-offs, it is needed to compare adaptive modulation with alternative implementations. Three algorithms are featured: (i) the no adaptation case (ii) adaptive modulation and (iii) an adaptive modulation and coding scheme. The channel parameters used for these simulations are summarized in Table3.1

**Table 3. 1: Channel parameters.**

| | |
|---|---|
| **Channel model** | **Flat fading** |
| **Doppler shift** | 70 Hz |
| **Correlation level** | Low |
| **Number Tx*Rx** | 2*2 |
| **Channel BW** | 20 MHz |
| **Data** | 10 Mbits |
| **Equalization mode** | ZF |
| **snrdB** | 17 dB |

### 3.2.1 No Adaptation

Our program uses a while loop that processes one subframe at a time. The simulation stops when the number of bits processed reaches the maximum number of bits, initially set to 10Mbits. For each subframe sent it reports, on the workspace, a set of parameters used and the results measured for the current transmission as shown in figure 3.3

```
Subframe                        = 1
Modulation                      = 64QAM
Instantanous Data rate          = 61.66 Mbps
Average Data rate               = 61.66 Mbps
Instantanous Modulation rate = 6.00
Average Modulation rate         = 6.00
Instantanous Coding rate        = 0.3333
Average Coding rate             = 0.3333
MIMO Antenna                    = 2 x 2
Bits processed                  = 123328
BER                             = 0.0403315
```

**Figure 3. 3: Report of parameters and measurments by subframe**

For the no adaptation case a fix coding rate of 1/3 is preferred and the same parameters early mentioned in table 3.1.

The results show in figure 3.4 are expected and well known. The Bit Error Rate is considerably small for low order modulations like QPSK and it goes higher as the modulation order increases as for the 64QAM modulation. It is quite well know that, for the same channel conditions, the probability of error increases as the modulation order increases due to the short distances between the modulated points in the constellation diagram.

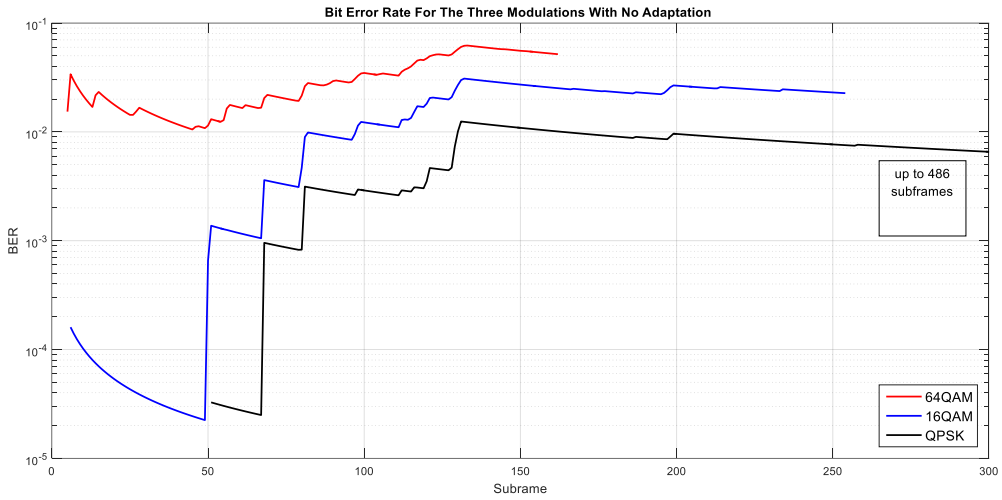


**Figure 3. 4: Bit Error Rate for the Three Modulations without Adaptation**

Eventually the number of Subrames thus the throughput is expected to go higher as the modulation order increases. For the case of QPSK modulation 2 bits are needed to encode each of its four different modulation symbols. The 16QAM uses 4 bits to encode 16 constellation points. The 64QAM modulation involves 64 different possible signalling values and thus requires 6 bits to represent a single modulation symbol. Which means that sending a

single symbol results in the transmission of 6 bits for 64QAM and therefore increasing the throughput.

However, as the channel becomes noisier, we should resort to use modulation schemes with more inter-symbol separation, such as QPSK. This in turn will reduce the number of bits per sample and reduce the throughput.

The table 3.2 below summarizes the average data rate, the Bit Error Rate and the number of subframes for each modulation according to the channel paramters initially presented in table3.1:

**Table3. 2: Number of subframes and average data rate for each modulation.**

| Type of Modulation | Average Data Rate (Mbps) | Average Bit Error Rate | Number of subframes |
|---|---|---|---|
| **QPSK** | 20.62 | 0.006063 | 486 |
| **16QAM** | 39.23 | 0.015130 | 255 |
| **64QAM** | 61.66 | 0.030400 | 163 |

Remarque: The number of subframes can be considered as the time needed to transmit this data. Where each subframe is 1 ms long and a single frame is composed of 10 subframes which is 10 ms long.

### 3.2.2 Adaptive Modulation

Let’s first use the CQI channel state reporting to dynamically change the modulation type of the current transmission. A wideband adaptation is applied where the modulation changes within each subframe.

Our program uses a while loop that processes one subframe at a time. The simulation stops when the number of bits processed reaches the maximum number of bits initially set 10Mbits. For each subframe sent it reports, on the workspace, a set of parameters used and the measured results for the current transmission as shown in figure 3.5. The channel parameters used are the same as for the no adaptation case (Table3.1) with a fixed coding rate of 1/3 and the modulation that changes according to the CQI criterion.

```
Subframe                        = 13
Modulation                      = 64QAM
Instantanous Data rate          = 61.66 Mbps
Average Data rate               = 54.20 Mbps
Instantanous Modulation rate = 6.00
Average Modulation rate         = 5.29
Instantanous Coding rate        = 0.3333
Average Coding rate             = 0.3333
MIMO Antenna                    = 2 x 2
Bits processed                  = 758768
BER                             = 0.00695865

---
Subframe                        = 14
Modulation                      = 16QAM
Instantanous Data rate          = 39.23 Mbps
Average Data rate               = 53.20 Mbps
Instantanous Modulation rate = 4.00
Average Modulation rate         = 5.20
Instantanous Coding rate        = 0.3333
Average Coding rate             = 0.3333
MIMO Antenna                    = 2 x 2
Bits processed                  = 798000
BER                             = 0.00661654
```

**Figure 3. 5: Parameters and measurements for each subframe**

Figure 3.6 illustrates the Bit Error Rate for the no adaptation and the adaptive modulation case. The green line represents the adaptive modulation results where it is clear how the adaptation of the modulation results in a stable BER as the data is been transmited.

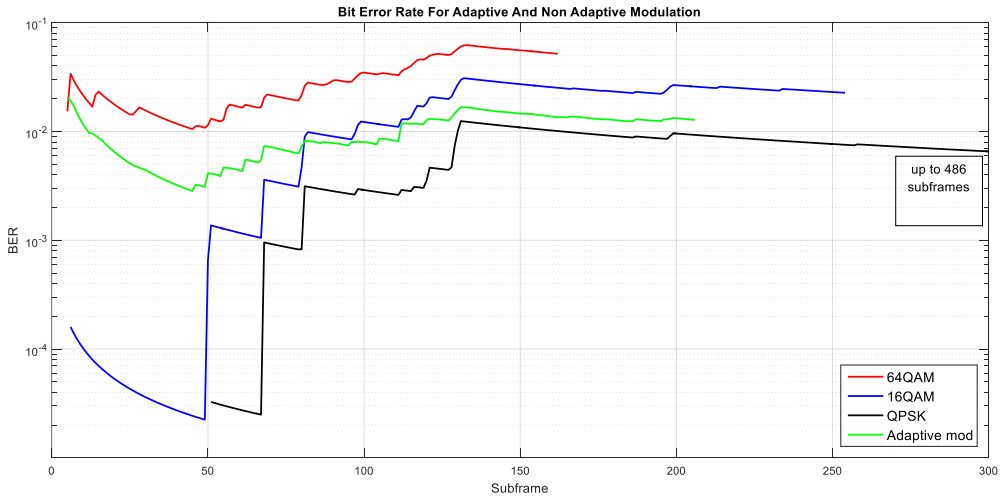


**Figure 3. 6: Bit Error Rate for adaptive and non-adaptive modulation**

Adapting the modulation gave us an average BER compared to the no adaptation case and also a significant improvement for the throughput as show in figure 3.7.

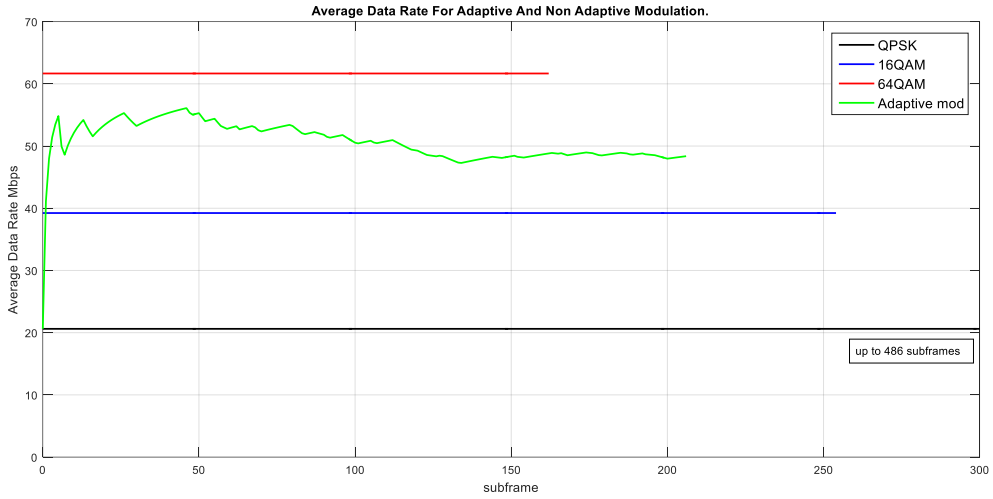


**Figure 3. 7: Average Data Rate for adaptive a non-adaptive modulation**

Remarque: The adaptive modulation system reduces the transmission errors and improves the average data rate. This improvement results in using the appropriate amount of subframes which give us an acceptable transmission time. These results are summarized in Table 3.3:

**Table3. 3: Results for the adaptive and non-adaptive modulation experiment.**

| Type of Modulation | Average Data Rate (Mbps) | Average Bit Error Rate | Number of subframes | Coding rate |
|---|---|---|---|---|
| **QPSK** | 20.62 | 0.006063 | 486 | 1/3 |
| **16QAM** | 39.23 | 0.015130 | 255 | 1/3 |
| **64QAM** | 61.66 | 0.030400 | 163 | 1/3 |
| **Adaptive** | 48.37 | 0.009719 | 207 | 1/3 |

As an example on how the SNR measured is mapped for a certain CQI index that gives the modulation type for each subframe the table 3.4 represent the SNR measured for each individual subframes and the corresponding CQI index found using the table2.1:

**Table3. 4: SNR to CQI mapping for adaptive modulation**

| Subframe number | SNR dB | CQI index | Modulation type |
|---|---|---|---|
| **5** | 12.654 | 11 | 64QAM |
| **6** | 1.023 | 5 | QPSK |
| **7** | 6.828 | 8 | 16QAM |
| **8** | 13.828 | 11 | 64QAM |

### 3.2.3 Adaptive modulation and coding

The CQI channel state reporting is used to determine both the modulation type and the coding rate by measuring the SNR of the channel and mapping it to the corresponding modulation and coding scheme as stated in the chapter two. This simulation takes advantage of these two characteristics of this channel reporting.

This time a comparison between a transmission with no adaptation and a one with both the adaptation of the modulation and the coding scheme is done. In order to be fair with the no adaptation case, a coding rate of 0.5 is set for each modulation order. While for the adaptive case the coding rate changes from 0.3 up to 0.95.

```
Subframe                    = 57
Modulation                  = QPSK
Instantanous Data rate      = 31.70 Mbps
Average Data rate           = 68.02 Mbps
Instantanous Modulation rate = 2.00
Average Modulation rate     = 4.62
Instantanous Coding rate    = 0.5880
Average Coding rate         = 0.5123
MIMO Antenna                = 2 x 2
Bits processed              = 3938784
BER                         = 0.0120075

---
Subframe                    = 58
Modulation                  = 16QAM
Instantanous Data rate      = 56.70 Mbps
Average Data rate           = 67.83 Mbps
Instantanous Modulation rate = 4.00
Average Modulation rate     = 4.61
Instantanous Coding rate    = 0.4790
Average Coding rate         = 0.5117
MIMO Antenna                = 2 x 2
Bits processed              = 3996120
BER                         = 0.0118352
```

**Figure 3. 8: Paramters and results for each subframe**

Our program uses a while loop that processes one subframe at a time. The simulation stops when the number of bits processed reaches the maximum number of bits initially set to 10Mbits. The parameters used and the measured results for each subframe are reported on the matlab workspace as shown in figure 3.8.

The channel parameters used are the same as for the no adaptation case and summarized the above mentioned Table 3.1.

Comment:

The figure 3.9 shows the Bit Error Rate for three transmission using a fixed modulation and a coding rate of **0.5**. Compared with the simulation using the Adaptation of these two parameters using the CQI reporting channel state. The transmission using the adaption shows a BER that is quite stable and with an averaged value compared to the baseline transmissions.

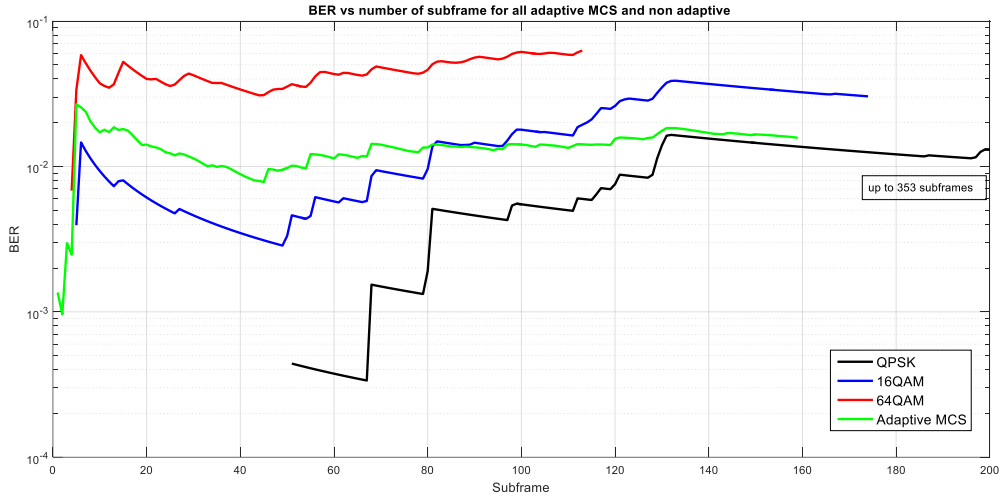


**Figure 3. 9: Bit Error Rate for adaptive modulation and coding rate with the no adaptation case**

These results show that this adaption technique using the CQI reporting reduces the bit error rate while improving the average data rate as shown in figure 3.10. This increase in data rate reduces the number of subframes needed to transmit this data, only 160 subframes, which reduces the transmission time.

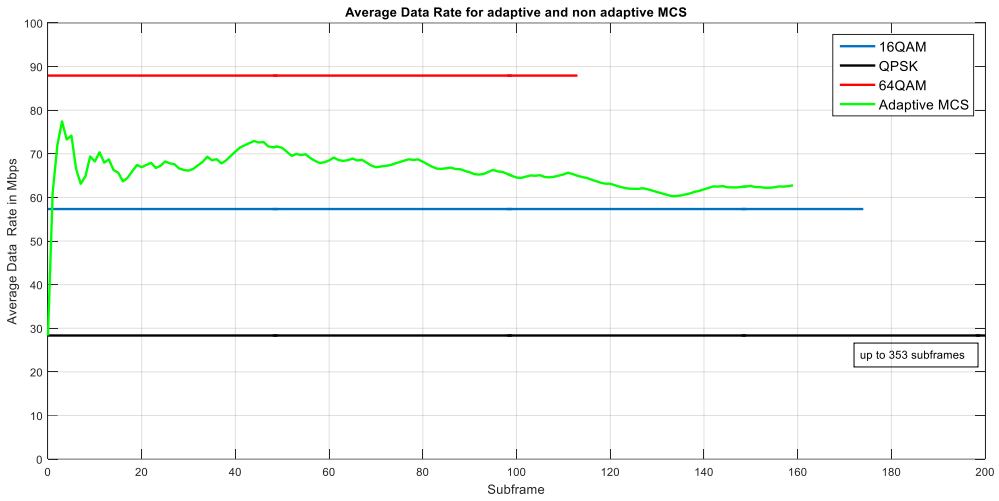


**Figure 3. 10: Average Data Rate for non-adaptive and adaptive modulation and coding scheme**

The table 3.5 summarizes the results discussed above:

**Table3. 5: Results for non-adaptive and adaptive modulation and coding scheme**

| Modulation type | Average data Rate in Mbps | Bit Error Rate | Coding Rate | Number Subframs |
|---|---|---|---|---|
| **QPSK** | 28.34 | 0.00796 | 0.5 | 353 |
| **16QAM** | 57.35 | 0.01689 | 0.5 | 175 |
| **64QAM** | 87.94 | 0.04362 | 0.5 | 114 |
| **Adaptive** | 62.78 | 0.01371 | 0.3 – 0.95 | 160 |

It is even possible to visualize the bit error rate for each subframe and its measured SNR.In Figure 3.11 illustrates the response of this adaptation for the measured BER compared to the SNR. The noise variations affect the BER for the first subframes then the adaptation takes place immediately to stabilize it around a reasonable value.

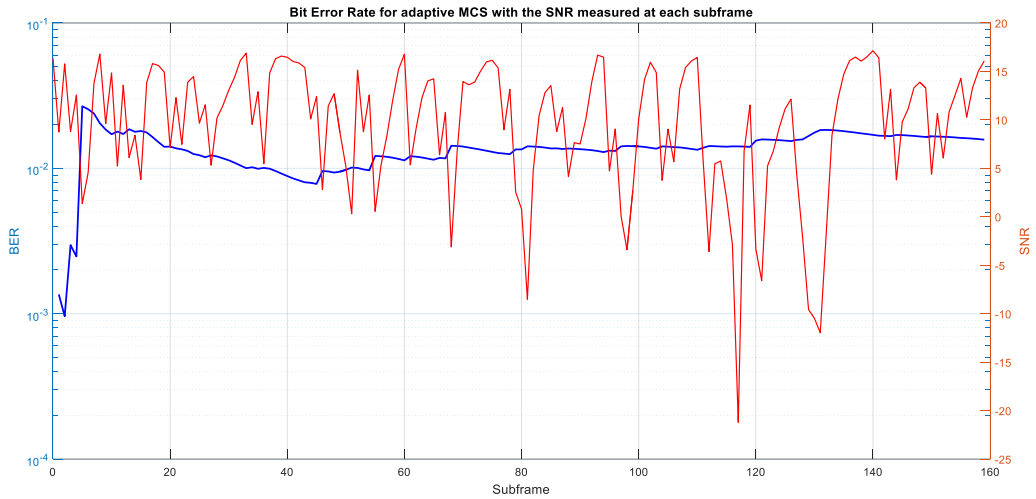


**Figure 3. 11: Bit Error Rate for adaptive MCS with the measured SNR for each subfram**

The table 3.6 below is an example showing the measured SNR for each subframe and its mapping to the corresponding CQI index that give the suited modulation and coding scheme:

**Table3. 6: SNR measured mapped to CQI index and modulation with coding rate**

| Subframe number | SNR in dB | CQI index | Modulation type | Coding Rate |
|---|---|---|---|---|
| **116** | 1.919 | 5 | QPSK | 0.4384 |
| **117** | -2.850 | 3 | QPSK | 0.3770 |
| **118** | -21.205 | 1 | QPSK | 0.0762 |
| **119** | 6.810 | 8 | 16QAM | 0.4785 |
| **120** | 11.530 | 10 | 64QAM | 0.4551 |

## 3.3 PMI and RI Based Adaptation

For this section an adaptation using the PMI channel state repotting will be performed alone and compared to a baseline no adaptation case. Then the RI estimation technique will be introduced and compared to the PMI case.

### 3.3.1 PMI Based Adaptation

For the adaptive Precoding Matrix Indicator a different set of parameters is used with and another channel model. Precoding works best with riche multipath channels. Therefor a 4*4 MIMO transceiver with the Extended Vehicular A (EVA 5 Hz) channel are implemented.

In fact what is interesting for us in this experiment is to demonstrate the added value of precoding using the PMI channel state reporting. Since for the 4*4 MIMO transceiver there are sixteen codebook indexes for the precoding matrix according to the standard. So this configuration has been taken into consideration for this section.

However, the Modulation and the coding rate remain fix where a 16QAM with a 1/3 coding rate are chosen respectively.

All the parameters are summarized in the following table3.7:

**Table3. 7: Channel parameters**

| **Channel model** | **EVA 5HZ** |
|---|---|
| **Doppler shift** | 5 Hz |
| **Correlation level** | Medium |
| **Number Tx*Rx** | 4*4 |
| **Channel BW** | 10 MHz |
| **Modulation type** | 16QAM |
| **Data** | 10 Mbits |
| **Equalization mode** | MMSE |
| **snrdB** | 30 dB |

Our program uses a while loop to process one subframe at a time, where a wideband adaptation is used. Each precoding matrix is computed by iterating through all PMI codebook entries; in other words, through a full search. The codebook index that minimizes the Mean Square Error MSE measure is the selected codebook index output.

The Figure 3.12 shows the bit error rate for an adaptive PMI based transmission and a no adaptation case.

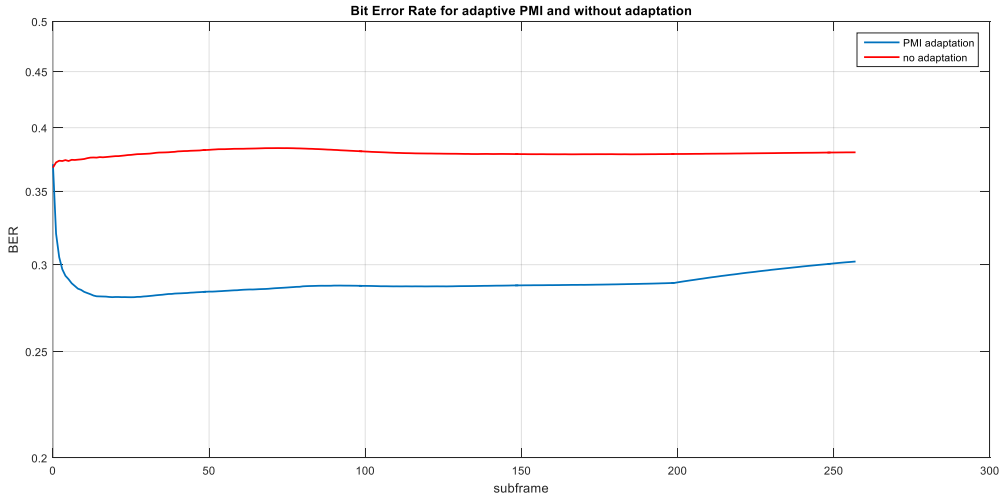


**Figure 3. 12: Bit Error Rate for adaptive PMI and no adaptation**

For the adaptative precoding matrix we have an improvement in the bit error rate whilst the average data rate remains the constant and equal to the case with no adaptation.

The table 3.8 below summarizes these results:

**Table3. 8: Results for adaptive PMI based simulation and the no adaptation simulation**

| Simulation type | Coding rate | Modulation type | Average data rate in Mbps | Bit Error Rate |
|---|---|---|---|---|
| **Baseline simulation no adaptation** | 1/3 | 16QAM | 39.82 | 0.3792 |
| **Adaptive precoding based on PMI feedback** | 1/3 | 16QAM | 39.82 | 0.2887 |

The results of the table 3.8 proves that by varying the precoding codebook index according to the channel condition, the system will produce less BER. Hence, it can be concluded that the performance for adaptive precoding based on PMI feedback simulation only improves the bit error rate comprared to case with no adaptation.

### 3.3.2 RI & PMI Based Adaptation

This section consist of two parts, the first one demonstrates the difference between the transmit diversity mode and the spatial multiplexing mode, then an adaptation using the RI estimation is shown to emphasis the advantages of using this technique. Also a comparison with the two fixed modes is given.

Part B deals with three experiments: the baseline with no adaptation, the PMI reporting based adaptation and finally an adaptation using a combination of both PMI and RI channel reporting states.

All the parameters used are summarized in table 3.9:

**Table3. 9: Channel parameters**

| | |
|---|---|
| **Channel model** | **EVA 5HZ** |
| **Doppler shift** | 5 Hz |
| **Correlation level** | Low |
| **Number Tx*Rx** | 4*4 |
| **Channel BW** | 20 MHz |
| **Modulation type** | 16QAM |
| **Data** | 10 Mbits |
| **Equalization mode** | MMSE |
| **snrdB** | 17 dB |

1. **Part A:**

Until now, only the transmission mode 4 closed loop spatial multiplexing has been introduced. This section discusses the advantage of using the RI estimation to switch the transmission mode from a mode 2 transmit diversity to a mode 4 spatial multiplexing.

First a comparison is done between a fixed mode 2 transmit diversity and a fixed mode 4 spatial multiplexing, then the RI estimation technique is used to switch over the two modes during the transmission in order to see the utility of using this technique rather that the fixed classical one.

The figure 3.13 illustrates the bit error rate for the fixed mode 2 transmit diversity and the fixed mode 4 spatial multiplexing.

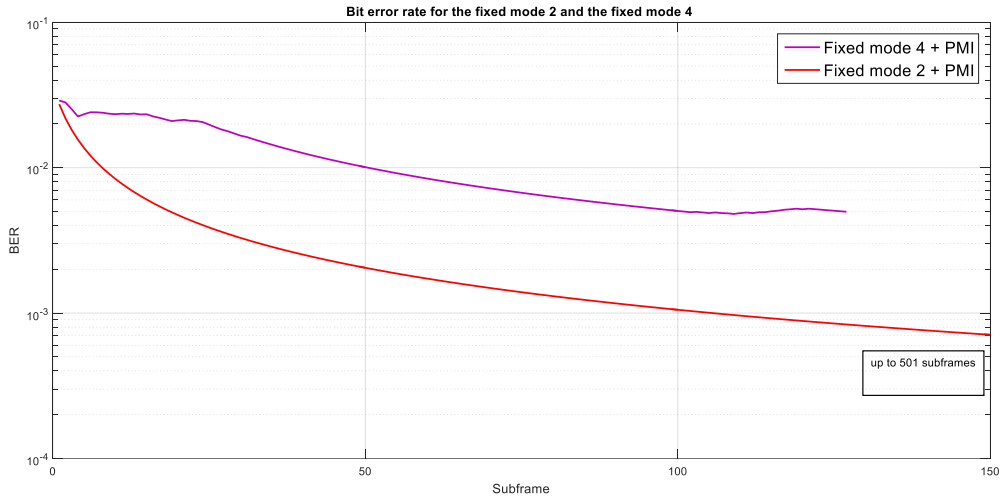


**Figure 3. 13: Bit Error Rate for the fixed mode 2 transit diversity and the fixed mode 4 spatial multiplexing**

And figure 3.14 illustrates the average data rate for the two transmission modes:

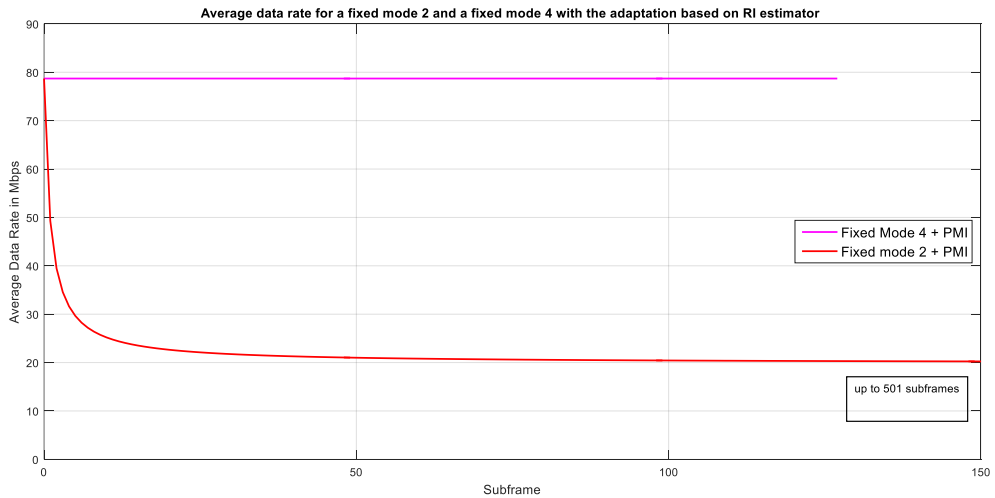


**Figure 3. 14: Average Data Rate for the fixed mode 2 transit diversity and the fixed mode 4 spatial multiplexing**

As it is illustrated on the above figures mode 2 transmit diversity is a more redundant mode hence it produces less BER than the spatial multiplexing mode 4. However the average

data rate is highly affected and the transmission time is longer compared to the spatial multiplexing mode.

The table 3.10 summarizes these results:

**Table3. 10: Results for the mode 2 transmit diversity and mode 4 spatial multiplexing**

| Transmission Mode | Average Data Rate in Mbps | Bit Error Rate | Number of subframes |
|---|---|---|---|
| **Transmit diversity mode 2** | 19.97 | 0.00107 | 501 |
| **Spatial multiplexing mode 4** | 78.7 | 0.01095 | 127 |

Using the RI estimation channel state the transmission mode switch from mode 2 to mode 4 and vice versa. The impact of this adaptation on the bit error rate is shown in figure 3.15 and compared to the fixed mode 2 and 4:

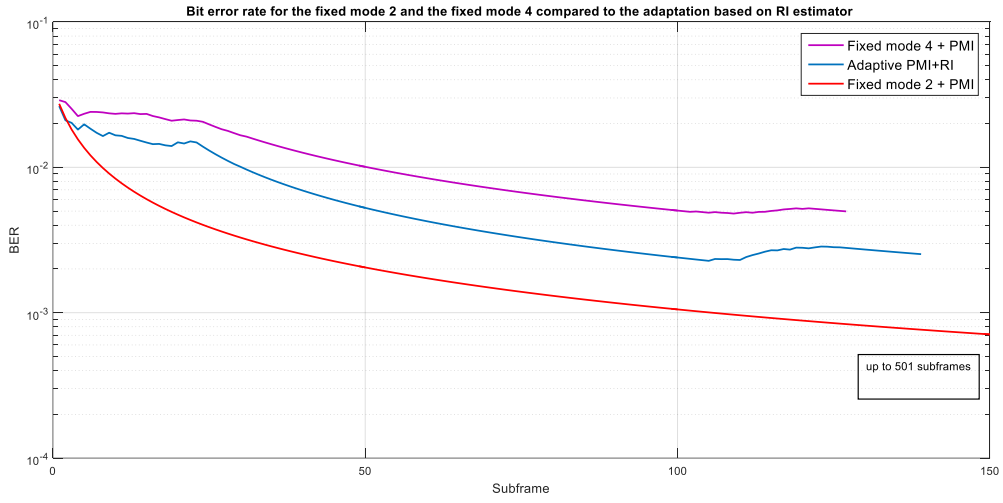


**Figure 3. 15: Bit Error Rate for the fixed mode 2 and the fixed mode 4 with the adaption RI based**

The figure 3.16 shows the average data rate for the fixed mode 2 and 4 compared to the adaptive case:

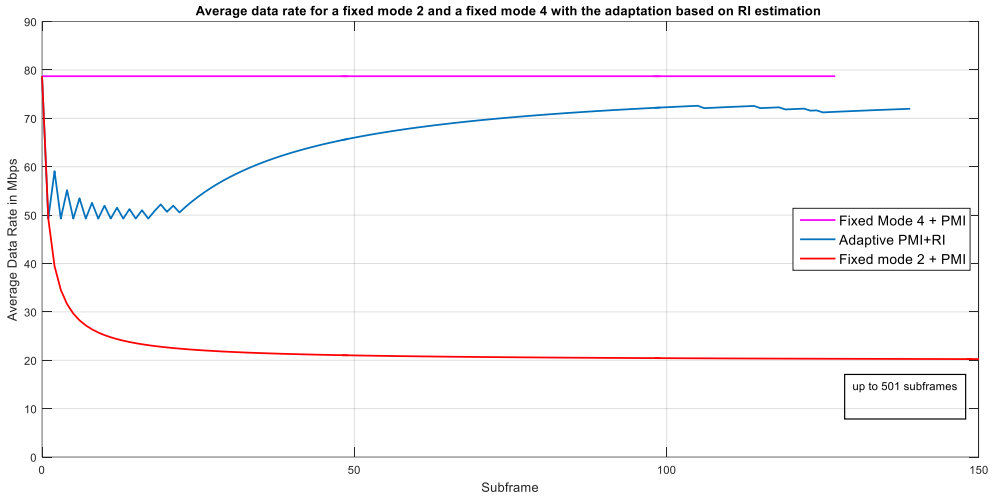


**Figure 3. 16: Average Data Rate for the fixed mode 2 and the fixed mode 4 with the adaption RI based**

The above two figures show the trade-off that is taken in consideration to implement this adaptation for the transmission mode. This results in a gain in the throughput whilst minimizing the bit error rate compared to the use of a fixed configuration.

The results of this experiment are summarized in table 3.11:

**Table3. 11: Results for the two modes and the adaptatin based on the RI estimation**

| Transmission Mode | Average data rate in Mbps | Bit Error Rate | Number of subframes |
|---|---|---|---|
| **Transmit diversity mode 2** | 19.97 | 0.00107 | 501 |
| **Spatial Multiplexing mode 4** | 78.7 | 0.01095 | 127 |
| **Adaptive Transmission based on RI stimator** | 71.98 | 0.00630 | 140 |

## 2. Part B:

The purpose of this part is to highlight the added value of using the RI estimation compared to the case of using only the PMI based adaptation. A transmission with no adaptation is given as a reference for the two.

The figure 3.17 below shows the bit error rate of three transmission: adaptation based on the RI estimation and the PMI based adaptation and the last one is the no adaptation case.

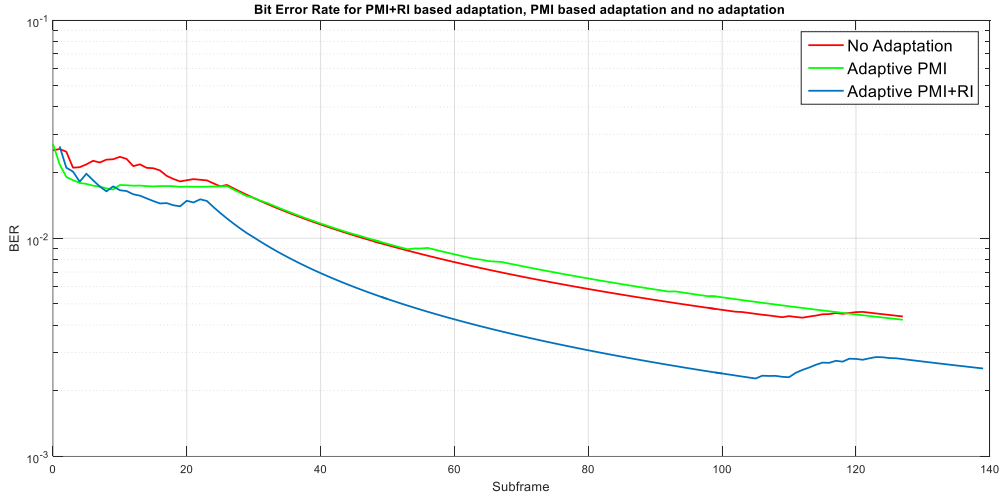


**Figure 3. 17: Bit Error Rate for the adaptation based PMI+Ri ,PMI based and no adaptation**

The average data rate reported is illustrated in figure 3.18 for the three cases:

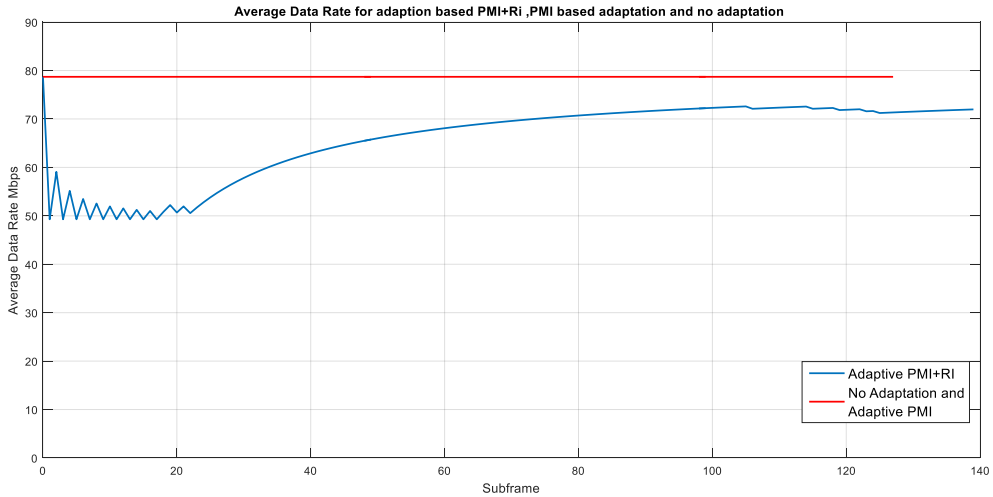


**Figure 3. 18: Average Data Rate for PMI+RI based adaptation, PMI based adaptation and no adaptation**

Since the transmission mode for PMI based adaptation is the spatial multiplexing mode 4 and remains the same for the whole transmission we expect the average data rate to be equivalent to the no adaptation case. Whereas for the RI+PMI adaptation there is an improvement on the bit error rate compared to the PMI based adaptation alone whilst the average data rate in this case is affected by the changes in the transmission mode but still reaches a satisfactory level.

The table 3.12 summarizes these results:

**Table3. 12: Results for PMI+RI adaptation, PMI adaptation and no adaptation case**

| Transmission Mode | Average Data Rate in Mbps | Bit Error Rate | Number of subframes |
|---|---|---|---|
| **No adaptation mode 4** | 78.7 | 0.01121 | 127 |
| **PMI based Adaptation mode 4** | 78.7 | 0.00989 | 127 |
| **RI+PMI based adaptation** | 71.98 | 0.00630 | 140 |

The PMI based adaptation isn’t sufficient by its own. In fact, it provide a small improvement in the bit error rate compared to the no adaptation case. Therefore a combination of the RI estimation and the PMI based adaptation is implemented reduce even better the bit error rate at the cost of having a small loss for the throughput and a slightly longer transmission with 13 additional subframes.

## 3.4 Adaptation Based on CQI, PMI and RI

The Link Adaptation system can now be implemented using the three main channel state discussed in the previous sections can be.

Our program uses a while loop to process one subframe at a time. The simulation stops when transmission reaches the maximum number of bits given. It applies a wideband adaptation that allows the system to adapt the transmission parameters over each individual subframe.

The first simulation uses a 2 by 2 transceiver then a 4 by 4 will be used.

The parameters chosen for the 2 by 2 simulation are summarized in table 3.13:

**Table3. 13: Channel parameters for a 2*2 transceivers**

| | |
|---|---|
| **Channel model** | Frequency selective |
| **Doppler shift** | 70 Hz |
| **Correlation level** | Medium |
| **Number Tx*Rx** | 2*2 |
| **Channel BW** | 20 MHz |
| **Data** | 10 Mbits |
| **Equalization mode** | MMSE |
| **snrdB** | 20 dB |

The bit error rate for this channel with its measured SNR for each subframe is shown in figure 3.19:

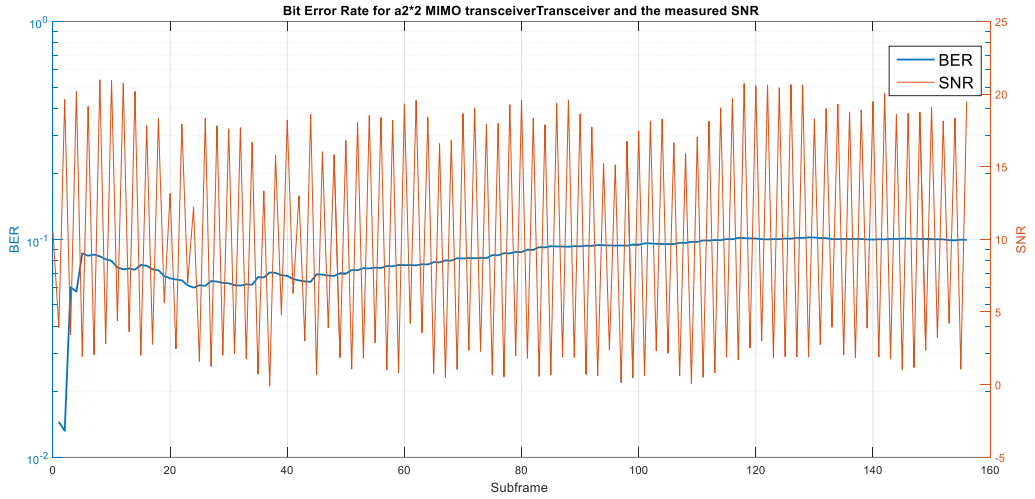


**Figure 3. 19: Bit Error Rate for a2*2 MIMO transceiverTransceiver and the measured SNR**

The figure 3.20 show the average data rate with its measured SNR for each subframe:

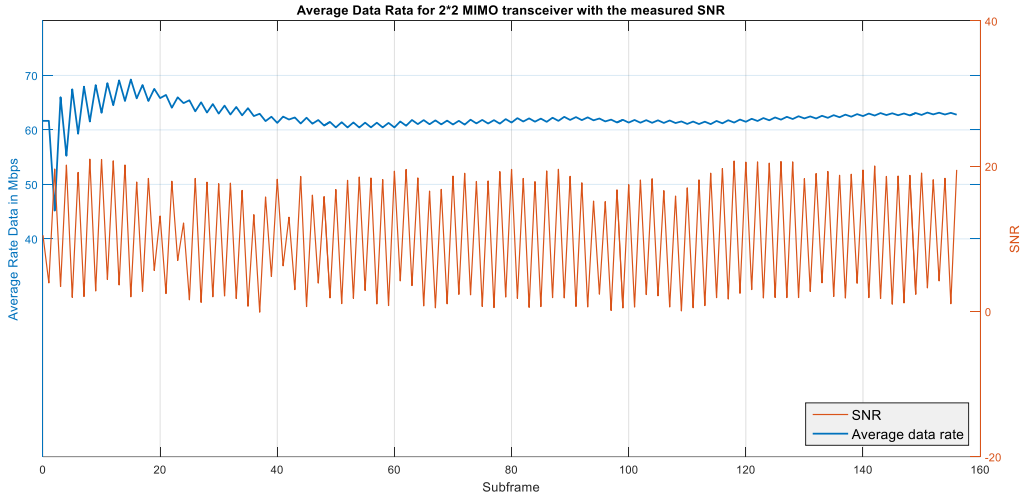


**Figure 3. 20: Average Data Rata for 2*2 MIMO transceiver with the measured SNR**

As the data is been transmitted the SNR is measured and shown here to emphasize the behaviour of the transmission with respect to it. The previous two figures show the stability of the bit error rate and the average data rate despite the changes in the SNR.

To investigate the response of the 4*4 MIMO transceiver with the following channel parameters have been used:

**Table3. 14: Channel parameters for the 4*4 transceiver**

| | |
|---|---|
| **Channel model** | Flat fading |
| **Doppler shift** | 70 Hz |
| **Correlation level** | Low |
| **Number Tx*Rx** | 4*4 |
| **Channel BW** | 20 MHz |
| **Data** | 10 Mbits |
| **Equalization mode** | MMSE |
| **snrdB** | 30 dB |

The figure 3.21 represents the bit error rate for the 4*4 transceiver with its measured SNR for each subframe:

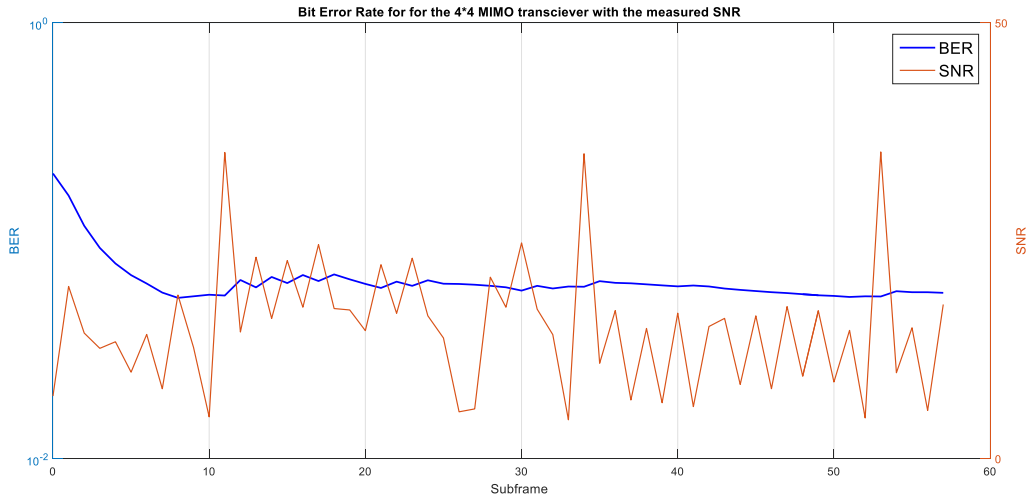


**Figure 3. 21:Bit Error Rate for the 4*4 MIMO transceiver the measured SNR for each subframe**

The average data rate is illustrated in figure 3.22 with the instantaneous measured SNR for each subframe:

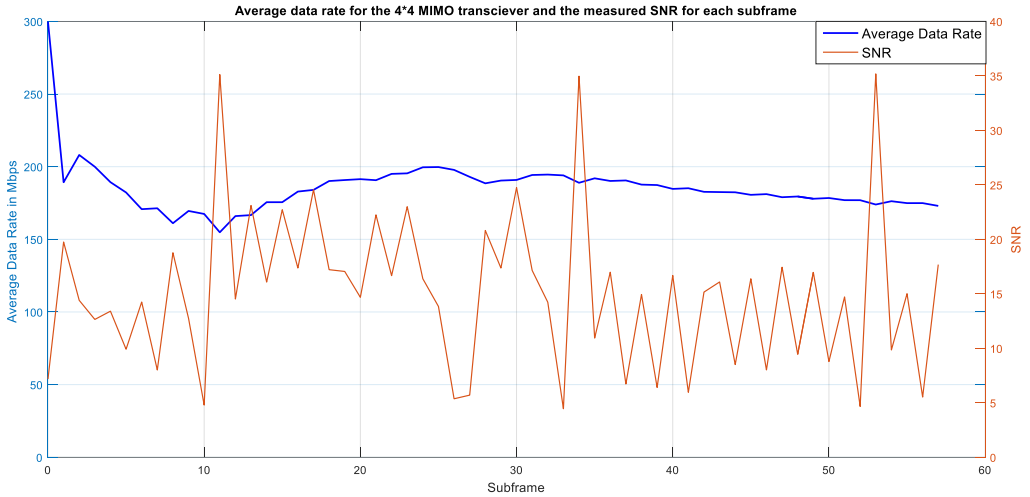


**Figure 3. 22: Average Data Rate for the 4*4 MIMO transceiver the measured SNR for each subframe**

The 4*4 MIMO transceiver is showing robustness against noise. During the transmission the SNR varies as shown by the previous two figures whilst the bit error rate and the average data rate show a resistance to this variations and keep a relatively stable values.

The table3.15 summarizes some parameters as they change for each subframe:

**Table3. 15: Results for the 4*4 MIMO transciever**

| Subframe number | SNR measured | RI Index | PMI index | CQI index | Modulation type | Coding rate |
|---|---|---|---|---|---|---|
| **26** | 13.837 | 4 | 10 | 11 | 64QAM | 0.5537 |
| **27** | 5.366 | 4 | 9 | 7 | 16QAM | 0.3691 |
| **28** | 5.699 | 4 | 9 | 7 | 16QAM | 0.3691 |
| **29** | 20.815 | 4 | 11 | 14 | 64QAM | 0.8525 |

The table above is a sample of four subframes from the previous simulation where we have a degradation of the SNR. At the level of the subframe number 27 an abrupt change in the SNR is measured and the channel stat reporting have been assigned different values from the previous ones. This induces a change in the modulation scheme and the coding rate to

give more robustness to the transmission and minimize the bit error rate. The system also choses a new precoding matrix indicated by the PMI index and it keeps the transmission mode 4 unchanged to maintain the data rate fix.

## 3.5 Results Summary

Adaptive modulation case

**Table3. 16: Comparative results for adaptive modulation**

| Comparison | Bit Error Rate comparison in percentage | Average Data Rate |
|---|---|---|
| **Adaptive case vs QPSK** | +37.62% (degradation) | +57.37% (improvement) |
| **Adaptive case vs 16QAM** | -35.76% (improvement) | +18.89% (improvement) |
| **Adaptive case vs 64QAM** | -68.02% (improvement) | -21.55% (degradation) |

Adaptive modulation and coding case:

**Table3. 17: Comparative results for adaptive modulation and coding**

| Comparison | Bit Error Rate comparison in percentage | Average Data Rate |
|---|---|---|
| **Adaptive case VS QPSK** | +42.67% (degradation) | +54.86% (improvement) |
| **Adaptive case vs 16QAM** | -18.83% (improvement) | +8.65% (improvement) |
| **Adaptive case vs 64QAM** | -68.57% (improvement) | -28.48% (degradation) |

Adaptive precoding based on PMI feedback:

**Table3. 18: Comparative results for adaptive PMI with no adaptation**

| Comparison | Bit Error Rate | Average Data Rate |
|---|---|---|
| **PMI based adaptation vs No adaptation** | -23.87% (improvement) | 0% |

Adaptation Based on RI estimation compared to the fix mode 2 and 4:

**Table3. 19: Comparative results for the fixed mode 2 and 4 with adaptive mode**

| Comparison | Bit Error Rate | Average Data Rate |
|---|---|---|
| **Adaptive vs Fixed transmission mode 2** | +83.01% (degradation) | +72.26 (improvement) |
| **Adaptive vs Fixed transmission mode 4** | -36.71% (improvement) | -8.54 (degradation) |

Adaptation based on PMI+RI compared to the PMI based one and the no adaptation case:

**Table3. 20: Comparative results for the PMI+Ri based adaptation**

| Comparison | Bit Error Rate | Average Data Rate |
|---|---|---|
| **Adaptive precoding vs no adaptation** | +11.78% (improvement) | 0% |
| **PMI+RI adaptation vs PMI adaptation** | +36.30% (improvement) | -8.53% (degradation) |

## Conclusion

The results are clear and speak of themselves, the link adaptation of the LTE standard has been implemented where it gives significant improvements on the overall transmission.

It happens that the system concedes over some losses in the bit error rate to gain in throughput or vice versa, where all of that is according to the user's needs and the channel transmission quality.

These techniques allow the system to take advantage of all the transmission parameters. It leads this wireless communication system to a new era of dynamic resources allocation.

## General Conclusion

The goal of this thesis was to investigate the link adaptation techniques of the LTE wireless communication system. The three main channel state reporting and their implementation have been taken into consideration. The performances of each one of them was compared to the classical methods. In order to emphasis the design trade off of this system.

The classical methods were first implemented to make a point about their divergences and characteristics. The adaptive modulation case was first carried out, it was found that this adaptation helped to improve the average data rate over a reasonable bit error rate. This led us to go to the next stage where an adaptation of the modulation and the coding rate was considered. This additional parameter gave to the system more control over the transmission to stabilize the bit error rate and improve the throughput.

A precoding based adaptation is a major enhancement in the LTE MIMO. In fact multipath fading has been minimized using the PMI channel state reporting which induced an improvement in the bit error rate whereas no changes were noticed on the average data rate.

The spatial multiplexing mode was preferred for the first simulation. However transmit diversity is also available as a transmission mode in the LTE system. The difference between the two modes has been presented. Transmit diversity gives more redundancy and robustness to the system that results in a low bit error rate reduces the average data rate for the spatial multiplexing a maximum data rate is achievable with a degradation in the bit error rate

The RI estimation gives to the system the ability to switch over the two modes and takes advantages of all the network abilities. The use of the RI estimation allowed a gain in the data rate and produced an acceptable bit error rate.

The combination of these techniques resulted in a complete and fully functional link adaptation scheduling system. It has been tested over a 2 by 2 and a 4 by 4 MIMO transceivers. The results of the bit error rate have shown a stable and a robust response over the changes in the measured instantaneous SNR. In addition to that, high data rate transmissions have been achieved.

Finally we can conclude that this set of techniques for the link adaptation permits to take advantage of all the network resources, to gain in transmission efficiency and improve the user experience.

## Future Work

As an extension to this work it will be interesting to investigate the response of this link adaptation over the multitude of channel parameter required by the standard.

We suggest to further investigate the subband adaptation. Since it has been recommended to offer a better control over the network resources.

As a more optimistic point one can consider a multi user transmission and implement a large scale adaptation. Eventually cell edges related problems can be taken into consideration.

## References

[1] 3GPP; TSG RAN; High Speed Downlink Packet Access (HSDPA); Overall description; Stage 2 (Release 5), 3GPP TS 25.308 Version 5.7.0, URL valid as of September 08 2009: **http://www.3gpp.org/ftp/Specs/html-info/25308.htm**

[2] 3GPP; TSG RAN; FDD Enhanced Uplink; Overall description; Stage 2 (Release 6), 3GPP TS 25.309 Version 6.6.0, URL valid as of September 08 2009: **http://www.3gpp.org/ftp/Specs/html-info/25309.htm**

[3] D. Gesbert, et.al, "From Theory to Practice: An overview of MIMO space-time coded wireless systems", IEEE Journal On Selected Areas In Communications, Vol. 21, No. 3, April 2003.

[4] E. Telatar, "Capacity of Multi-Antenna Gaussian Channels," technical memorandum, AT&T Bell Laboratories, June 1995.

[5] G.J. Foschini and M.J. Gans, "On limits of wireless communications in a fading environment when using multiple antennas," Wireless Personal Communications, vol. 6, pp. 311-335, March 1998.

[6] Dahlman, E. Parkvall, S. Sköld, J. Beming, P., 3G Evolution: HSPA and LTE for Mobile Broadband, Elsevier, Second edition, 2008

[7] 3GPP TS 36.211 V8.5.0 (2008-12), "Evolved Universal Terrestrial Radio Access (E-UTRA) Physical Channels and Modulation (Release 8)".

[8] Touheed, H., Quddus, A.U., Tafazolli, R., An Improved Link Adaptation Scheme for High Speed Downlink Packet Access, Vehicular Technology Conference 2008, IEEE, May 2008, pp. 2051-2055

[9] J. Fan, Y. Qinye, G. Y. Li, B. Peng, and Z. Xiaolong, "MCS Selection for Throughput Improvement in Downlink LTE Systems," in Computer Communications and Networks (ICCCN), 2011 Proceedings of 20th International Conference on, 2011, pp. 1-5

[10] Martin-Sacristan, D. Monserrat, J.F. Calabuig, D. Cardona, N., HSDPA Link Adaptation Improvement Based on Node-B CQI Processing, 4th Internation Symposium on Wireless Communication Systems, IEEE, Oct 2007, pp 597-601

[11] David A E, Furuskär A, Jading Y, Lindström M and Parkvall S 2009 LTE: the evolution of mobile broadband IEEE Communications Magazine p 45.